

A STUDY OF POLYURETHANE POLYMERIZATION
VIA MODELING AND EXPERIMENT

A Thesis
presented to
the Faculty of the Graduate School
at the University of Missouri-Columbia

In Partial Fulfillment
of the Requirements for the Degree
Master of Science

by
WANG, HUAQI
Dr. Galen Suppes, Thesis Supervisor

MAY 2014

© Copyright by Huaqi Wang 2014

All Rights Reserved

The undersigned, appointed by the dean of the Graduate School, have examined the thesis entitled.

STUDY OF POLYURETHANE POLYMERIZATION VIA
MODELING AND EXPERIMENT

presented by Wang, Huaqi,

a candidate for the degree of master of science,

and hereby certify that, in their opinion, it is worthy of acceptance.

Professor Galen Suppes

Professor Paul Chan

Professor Fu-Hung Hsieh

ACKNOWLEDGEMENTS

I would like to thank Professor Galen Suppes' for his advice and guidance for these two years. His help was instrumental in my change from an undergraduate to a qualified researcher. Thanks to Drs. Paul Chan and Fu-Hung Hsieh's for their advice and suggestions about my research and defense. Their advice improves the accuracy and logic of my research.

Also, thanks for help from PhD students Yusheng Zhao, Rima Ghoreishi and Harith H. Al-Moameri and master students Zhong Fu and Yingyue Li on topics of experimental and modeling techniques during two years. I am honored to work together with such excellent students like them. Thanks for University of Missouri for providing me a good academic atmosphere and economic support.

Finally, thanks to my parents support from mental aspect and economical aspect. I could not have accomplished my master degree without your help. The education you helped me attain will accompany me for a lifetime.

TABLE OF CONTENTS

ACKNOWLEDGEMENTS.....	ii
TABLE OF CONTENTS.....	iii
LIST OF ILLUSTRATIONS.....	v
LIST OF TABLES.....	vii
ABSTRACT.....	viii
Chapter 1. Introduction.....	1
Chapter 2. Modeling and validation of isocyanate profiles during polyurethane polymerization reaction.....	3
2.1 Introduction.....	3
2.2 Experiment.....	10
2.3 Modeling.....	13
2.4 Result and Discussion.....	15
2.5 Conclusion.....	28
2.6 Acknowledgements.....	28
Chapter 3. Resin from natural oil.....	29
3.1 Introduction.....	29
3.2 Background – Natural Oils.....	31
3.3 Background – Natural Resin Polymerization.....	37
3.4 Simulation of Polymerization.....	39

3.5 Equation using in Matlab	40
3.6 Experimental Studies and Verification of Model	47
3.7 Simulation results.....	49
Chapter 4. Future study	53
Bibliography	54

LIST OF ILLUSTRATIONS

Figure 1. Isocyanate reaction profile with fitted model for reaction of 1-pentanol with PMDI at an isocyanate index =2.0 without catalyst.....	15
Figure 2. Isocyanate reaction profile with fitted model for reaction of 2-pentanol with PMDI at two isocyanate indices isocyanate indices. Symbols “▲” and “■” represent average experiment data of isocyanate indices of 1.1 and 2.0.	16
Figure 3. Extended time isocyanate reaction profile with fitted model for reaction of 1-pentanol with PMDI at 80 °C with different catalysts. C ₁₅ is the concentration of isocyanate functional groups after 15 min of reaction. Symbols “▲”, “■”, “●”, “×” and “◆” represent experiment data with UL22, UL29, Cat5, Cat8 and blank control.	18
Figure 4. Isocyanate reaction profile with fitted model for reaction of 1-pentanol with PMDI at 4 catalysts at 110 °C. Symbols “▲”, “■”, “●”, “×” and “◆” represent experiment data with UL22, UL29, Cat5, Cat8 and blank control.	19
Figure 5. Isocyanate reaction profile with fitted model for reaction of V360 with PMDI at an isocyanate index=1.1 with a catalyst of cat8 at 0.12gram.....	20
Figure 6. Isocyanate reaction profile with fitted model for reaction of 76-635 with PMDI at three isocyanate indices. Symbols “▲”, “■” and “◆” represent experiment data with isocyanate index=2.0, 1.5 and 1.1.	22
Figure 7. Isocyanate reaction profile with fitted model for reaction of 1-pentanol and Epoxy oil with PMDI at different temperature. Symbols “×” and “■” represent experiment data of reaction without any catalyst at 80°C and 110°C. “●” and “◆” represent experiment data with Cat8 at 80°C and 110°C.....	23
Figure 8. Isocyanate reaction profile with fitted model for reaction of 1-pentanol and Epoxy oil with PMDI at different temperature. Symbols “×” and “■” represent experiment data of reaction without any catalyst at 80°C and 110°C. “●” and “▲” represent experiment data with Cat8 at 80°C and 110°C. Dash line represent model without acceleration.....	25
Figure 9. Market volume by kinds.....	30
Figure 10. Typical lab experiment polymerization device.	31

Figure 11. Caster oil (triricinolein)	33
Figure 12. Soybean oil	34
Figure 13. Tung oil [22].....	35
Figure 14. Linseed oil.	35
Figure 15. Example polymer structures[23].	36
Figure 16. Program algorithm.....	42
Figure 17. Example simulation output-Monomer profiles.	49
Figure 18. Example simulation output-Carbon-carbon double bonds profiles.....	50
Figure 19. Example simulation output-Temperature profiles.....	51
Figure 20. Example simulation output-Degree of polymerization profiles.	52

LIST OF TABLES

Table 1. Summary of impact of potential reaction products.....	7
Table 2. Gel reaction formulation of using 1-pentanol or with epoxy as B-side at isocyanate index=2.0.	10
Table 3. Kinetic parameters of main reaction without catalysis which has been justified.	17
Table 4. Kinetic parameters of main reaction with cat8 (Dimethylcyclohexylamine) which has been justified.	17
Table 5. Kinetic parameters of urethane functional groups reaction with isocyanate functional group.....	20
Table 6. Kinetic parameters of epoxy functional groups reaction with isocyanate functional group.....	27
Table 7. Typical fatty acid compositions of selected plant oil. ^a [21].....	32
Table 8. Typical fatty acid compositions compare form.	33
Table 9. Catalysts used by the experiment.....	37
Table 10. Summary of typical monomers and applications.....	38
Table 11. Classified fatty acid.	40
Table 12. Simulation code.	42
Table 13. Typical recipe.	47
Table 14. Literature value of soybean oil reaction(Determination of Kinetic Parameters from Dynamic DSC measurement Using Kissinger's Equation).[32]	48
Table 15. Free Radical Scavenger Capacity of oil in lipidic phase at 180 °C.	48

A STUDY OF POLYURETHANE POLYMERIZATION
VIA MODELING AND EXPERIMENT

Huaqi Wang

Dr. Galen Suppes, Thesis Supervisor

ABSTRACT

This thesis is on the topic of modeling thermoset polymerization. More specifically, Chapter 2 is a detailed study of isocyanate concentration profiles with the goal of validating modeling work that was based on temperature profiles for polyurethane thermoset polymerization. Chapter 3 is on an extension of the modeling methods to resin polymerization of unsaturated vegetable oils.

On the work related to polyurethane thermoset polymerization, a Matlab program has been developed to model urethane foaming processes for the purpose of better understanding the foaming process and to advance simulation as a method to develop new foam formulations. As part of the verification of this model, isocyanate reaction profiles were followed for reactions with alcohol, urethane, and epoxy moieties.

The isocyanate concentration profiles were consistent with previously published reaction parameters for reactions of isocyanates with alcohols as well as reactions with the urethane moieties formed from reactions with alcohols. The data of this paper indicate that epoxy moieties react directly and indirectly with isocyanates to increase crosslinking. Epoxy moieties were reactive enough to impact temperature profiles during the first few

minutes of reaction. Both isocyanate-epoxy and isocyanate-urethane reactions can increase cross-linking during the hours following the initial foaming process.

Methodology which was used for polyurethane study has been expanded to vegetable oil self-polymerization. The vegetable oil reactivity has been analyzed. A model of carbon-carbon double bond reaction between vegetable oil and its copolymer has been established. Reasonable modeling results and theory have been developed. On the topic of the resin polymerization of unsaturated vegetable oils, Chapter 3 presents a summary of the reaction chemistry.

Chapter 1. Introduction

Polyurethanes were first made by Otto Bayer and his coworkers at I.G. Farben in Leverkusen in 1937. After decades of development, polyurethane has become one of the most popular polymers in the world. It is widely used in thermosetting polymers due to its excellent insulation properties.

A polymer comprised of a chain of organic units connected by urethane functional groups can be considered as polyurethane. Urethane functional groups are generated by reactions of isocyanate functional groups and hydroxyl functional groups.

In industry, MDI (Methylene diphenyl diisocyanate), pMDI (Polymeric methylene diphenyl diisocyanate) and TDI (Toluene diisocyanate) provide isocyanate functional groups. The functionality typically varies from two to three.

These studies are limited to the use of PMDI which tends to be less volatile than alternatives. As a result, the propensity to develop a sensitivity to handling PMDI at room conditions tends to be less.

Although polyurethane has been manufactured for decades; some problems have not been solved. Specifically, the study of side reactions that occur during polymerization need to be better understood to advance the science to the point where they can be meaningfully included in the simulation of polyurethane forming processes.

The experimental focus of this thesis is on side reactions involving isocyanates which is studied both from the perspective of experimental data and computer modeling.

A broader aspect of the work of this thesis is on the understanding and modeling of thermoset polymerization processes. An introduction to this topic as well as initial results on the modeling of this system is presented in Chapter 3.

Chapter 2. Modeling and validation of isocyanate profiles during polyurethane polymerization reaction

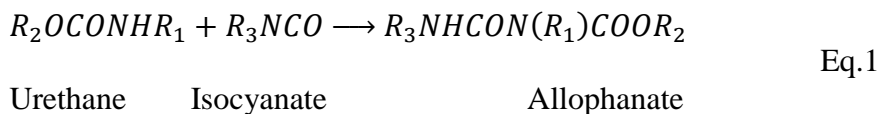
2.1 Introduction

Characterizing polyurethane reactions is more complex than most polymerization systems due the monomers having multiple reaction moieties, the large number of parallel reactions that can occur, and the hundreds of different oligomer and polymer products formed as reactions go to completion. Except for a small subcategory of thermoplastic polyurethanes, most urethane-forming processes are performed in batches that lead to a thermoset device/product.

This paper is on side-reactions that occur with isocyanate groups. In addition to increasing crosslinking and associated properties, these reactions consume any isocyanates that remain unreacted from the initial urethane-forming processes. The urethane-forming reaction is based around moieties of isocyanate and alcohol reacting to form urethane moieties. Isocyanate reactions with water, amines, and urethane moieties are the most common side reactions that occur. This paper also considers direct and indirect reactions where epoxy moieties react with isocyanate moieties. Reactions between isocyanates and either urethane or epoxy moieties tend to be more prominent when isocyanate groups are in excess (ie isocyanate indices greater than 1.0).

Duff and Maciel [1] demonstrated that side reactions can play an important part in polymer crosslinking. They demonstrated that isocyanate groups continue to react after all the alcohol is consumed and that the reactions impact the polymer properties.

As summarized by equation 1, urethane moieties react with isocyanates to form allophanates. Equation 1 is a more prominent reaction that can occur.



Singh and Boivin [2] found when the dimer of 2,4-tolylene diisocyanate was reacted with alcohols at about 90°C, the corresponding diurethanes were formed, giving only traces of allophanates. Higher temperatures in the range of 125°C to 160°C and catalysts such as triethylamine and N-methyl imorpholiile appeared to be necessary for the formation of allophanates.

Querat [3] found that allophanate formation can be catalyzed by dibutyltindilaurate, but dissociation occurs at high temperature. The rates of dissociation of allophanates are also affected by the nature of the nucleophilic agent (alcohol, amine).

Kogon [4] reports the allophanate-forming reaction as having a rate constant of 4.3×10^{-6} l/mol/s at an isocyanate index of 12.6 and temperature of 143 °C for reactions with isocyanate moieties on the polymer. For isocyanate monomers, the rate constant was reported as 1.017×10^{-5} - 6.5×10^{-6} l/mol/s at 106 °C -137°C.

Schwetlick and Noack [5] reported a 6.25% conversion of initial isocyanates in 5 minutes at an isocyanate index of 1.6 and temperature of 50°C. They used phenyl isocyanate and butanol as reagents in acetonitrile solvent with N,N-dimethylcyclohexylamine catalyst.

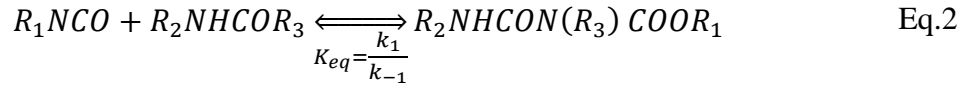
Heintz et al [6] observed 5.2%-7.9% conversion by side reactions at temperatures between 122 °C and 145 °C. They used ¹H NMR spectroscopy at 108 °C to detect

allophanate nitrogen present as 1.8% of the sample's nitrogen content. Lapprand et al [7] identified that allophanates comprised 10% of the total product after 1hr of reaction at 170°C and an isocyanate index of 1.

Spirkova et al [8] evaluated allophanate formation with dibutyltin dilaurate catalyst at 6×10^{-5} mol/l. The reaction rate was 0.21×10^{-6} l/mol/s at 90 °C and 2.22×10^{-6} l/mol/s at 120 °C at an isocyanate index of 3.0.

Vivaldo-Lima et al [9] used a model to study the polymerization process where the rate of allophanate generation was proportional to the urethane-forming reaction.

If water is in the system (e.g. as a to generate gas blowing agents), water reacts with isocyanates to form urea, and the isocyanate can then further react with the urea according to Equation 2.

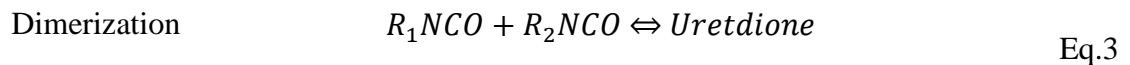


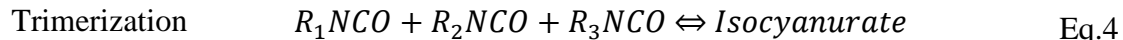
Isocyanate Urea Biuret

This reaction tends to be equilibrium limited ([10]). For systems with low reagent water contents, urea formation and reaction (equation 2) is negligible.

Dusek found [11] side reactions occur when isocyanate is in excess with selective catalysts. Initially, the formation of biuret was faster than allophanate.

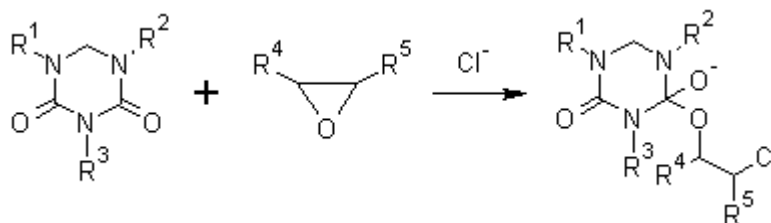
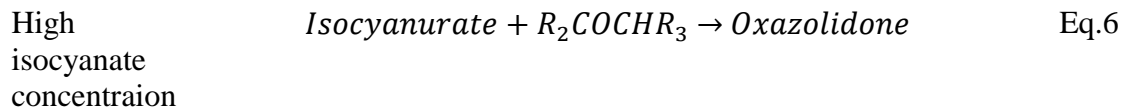
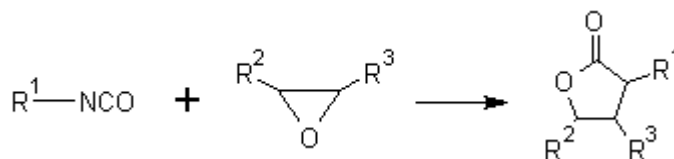
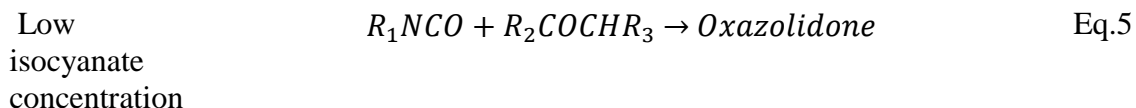
Delebecq, E., et al. [10] have shown that isocyanate groups undergo homocyclization in addition to forming allophanates which is characterized as dimerization (Eq.3) and trimerization (Eq.4). These reactions happen at lower temperatures with the monomers favored at higher temperatures.



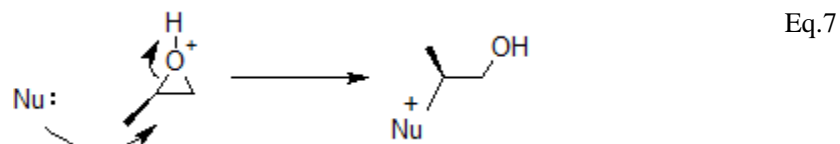


As with the biuret-forming reaction, these reactions are equilibrium limited. When competing with reactions that are not equilibrium-limited, the product mixes will eventually be dominated by those products that are not equilibrium limited.

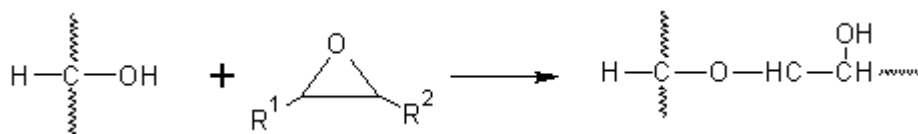
Recent work has shown that epoxy moieties can also participate in reaction networks of urethane formulations [12, 13]. Epoxy reactions are of particular interest for bio-based B-side components of urethane systems because they can be formed reliably and at lower cost from bio-oils like soybean oil. Little data are available on the rates and mechanisms of these reactions. Based on previous work [14, 15], the epoxy could react with isocyanate through two paths including reactions with the monomer (Eq. 5) and oligomers (Eq. 6).



Epoxy moieties also react with alcohols and water using nucleophilic substitution (e.g SN1) such as illustrated by Equations 7 and 8.



Eq.7



Eq.8

While the isocyanate-alcohol reaction takes place at reasonable rates at ambient temperature[16], the reactions of epoxy with alcohols require temperatures in excess of 100 °C for most commercial processes.

Table 1 summarizes reactions 1-8 including whether or not the product is equilibrium limited. The challenge of studying these reactions resides in the fact that there are multiple parallel reactions that can occur. The emphasis of this work is on the allophanate-forming reaction and the reactions with epoxy.

By performing reactions in systems free of water (gel reactions), biuret formation becomes negligible. The dimer and trimer forming reactions are of less interest since actual urethane form formulations will tend not to have a high excess of isocyanates, and so, for urethane plastics where most of the isocyanate reacts rapidly with alcohol, the remaining isocyanate can be reacted to extinction in the allophanate reaction.

The isocyanate-alcohol reaction will dominate the other reactions in urethane systems until the alcohols are substantially consumed (for isocyanate indices greater than 1). In the studies presented here the allophanate-forming reaction can be followed during the time period after the alcohol reacts.

Table 1. Summary of impact of potential reaction products.

Products	Equation	Conclusion	Source
----------	----------	------------	--------

Allophanate	Eq.1	Major byproduct that occurs if excess isocyanate is present.	[1] [2]
Biuret	Eq.2	Only present in systems where water is used in the formulation. It is equilibrium limited.	[2] [10] [11]
Uretdione Isocyanurate	Eq.3	Dimer and trimer of isocyanate that are equilibrium limited. High temperatures favor monomer. Is reacted to extinction as allophanate reaction proceeds.	[2] [10] [3]
Oxazolidone	Eq.5,Eq.6	Another main reason cause isocyanate consume when epoxy exist. Considered in this model and experiment.	[12]
Alcohol Product From Epoxy	Eq.7,Eq.8	Due to high reactivity of isocyanate alcohol reaction and isocyanate epoxy reaction. This reaction could be neglect in this system	[16]

Thus, the focus of this work is on reactions 1, 5, 6, 7, and 8. While these reactions have previously been studied, this work is on mixtures and with catalysts of particular interest to urethane formulations which are different than previously studied.

The works by Zhao and Ghoreishi [17, 18] placed a high emphasis on model development with robust experimental methods, primarily temperature profiles, to assist in model development based around isocyanate-alcohol reactions. Better understandings and more accurate data on the alcohol-isocyanate reactions provide an improved foundation for studying these other reactions. Use of temperature profiles is particularly insightful at time ranges of 5 to 500 seconds where the response time of the thermocouple is fast relative to the changes in temperature and where heat losses are relatively low as compared to heats of reaction.

The previous modeling work has been based on temperatures profiles; the objective of this work is to follow isocyanate concentration profiles to check the accuracy of modeling work to date and to provide insight into some of these other reactions. Use of

concentration profiles (via sampling and titration) is particularly useful at times scales greater than 5 minutes and specifically for reactions that are sufficiently slow to allow quenching and titration without the related time delays impacting the analyses.

2.2 Experiment

Gel reactions were performed based on the recipe of Table 2. Samples were collected and evaluated using the ASTM D2572-97(2010) standard to measure isocyanate concentrations in 1-1 g liquid samples. 1-pentanol and 2-pentanol were chosen as reagents to prevent gel formation and allow sampling at times up to 48 hours where typical urethane formulations would become solid and could not be titrated. Toluene was added as a diluent to limit the temperature increase of the reactions to temperatures more consistent with urethane systems (pentanols have lower heat capacities than typical urethane formulation polyols).

Table 2. Gel reaction formulation of using 1-pentanol or with epoxy as B-side at isocyanate index=2.0.

B-side Materials	Weight/g		Moles of functional groups	
	1-pentanol recipe	Epoxy recipe	1-pentanol recipe	Epoxy recipe
1-pentanol	11.50	11.500	0.130	0.130
Epoxy oil	0.000	3.000		0.013
Dimethylcyclohexylamine(Cat8)	0.120	0.120		
Momentive L6900	0.600	0.600		
T CPP	2.000	2.000		
A-side Material				
RUBINATE M	35.300	35.300	0.260	0.0260
Toluene (solvent)	10.440	10.440		
Isocyanate Index(NCO/OH)	-		2.000	2.000

As indicated in Table 2, the studies include formulations with epoxy moieties. The epoxy monomer was fully epoxidized soybean oil.

Gel reactions were performed as summarized by Zhao et al [18]. 1 gram samples were taken from the reaction mixture with 30 ml of dibutylamine-toluene used to quench

the reaction by both dilution and temperature reduction. The mixture was titrated within 15 minutes after the quench.

Chemicals used in the experimental include: 0.1mol/L HCL solution, 0.1mol/L Dibutylamine – toluene solution, 0.1g/L Bromphenol blue, Standard Polymeric MDI(Huntsman), Poly G76-635 (Arch Chemical, part of Lonza), Voranol 360(DOW),Vikoflex 7170 epoxidized soybean oil Momentive L6900, TRIS(CHLOROISOPROPYL) PHOSPHATE, Cat8 (DMCHA, Dimethylcyclohexylamine), Cat5 (PMDETA, N,N,N',N'',N''-pentamethyldiethylenetriamine), UL29 (Dioctyltin bis(2-ethylhexyl thioglycolate), and UL22(Dimethyltin mercaptide).

During extended-time studies, the reaction is allowed to proceed about 15 min in a beaker at near-adiabatic conditions which commonly results in a peak temperature of about 130 °C at 3 minutes into the reaction. After the initial 15 minutes of reaction, the alcohol has substantially reacted and heat losses exceed any heat of reaction. Then, 1-2 gram samples are placed in test tubes which are place in an oven at the temperature for extended studies. The samples are removed at 1hr, 12hr, 24hr and 48hr and titrated to detect isocyanate content.

Equations 9 and 10 are used to convert the volume of titrant to NCO content.

$$w_{NCO} / \% = \frac{(V_0 - V) \times c \times 4.202}{m} \quad \text{Eq.9}$$

$$\text{Total NCO} = \frac{w_{NCO}\% \times \text{Total weight}}{42.02} \quad \text{Eq.10}$$

Where

V_0 blank compare sample consumed Hydrochloric acid(mL)

V sample consumed Hydrochloric acid(mL)

c concentration of Hydrochloric (mol/L)

m sample weight (g)

During the initial 3 minutes of reaction, temperature profiles are followed for the epoxy reactions. Relatively low heat transfer coefficients and relatively high heats of reaction allow these temperature profiles to be used to characterize the reaction kinetics.

Previous modeling work has provided rate constants and heat transfer coefficients which are able to characterize the isocyanate-alcohol reactions. These results provide a starting point for characterizing the reaction. Two approaches distinguish the reactions of this study from the already-characterized isocyanate-alcohol reactions. For time periods greater than 15 minutes and an isocyanate index of 2.0, the alcohol has reacted less than detectable limits and changes in isocyanate concentrations can be attributed to the reactions of Table 1. At times less than 15 minutes, reaction temperature profiles are compared to control experiments with rigor placed on statistically significant increases in temperature that can be attributed to epoxy-related reactions.

2.3 Modeling

The isocyanate-alcohol gel reaction is modeling by using Zhao's work[18]. For this study additional equation and model is needed. Assuming reactions Eq.1 and Eq.6 are elementary, the rate expressions of equations 11 and 12 result. t

$$r_1 = [NCO] \times [Urethane] \times A_1 \times e^{-\frac{Ea_1}{RT}} \quad \text{Eq.11}$$

$$r_6 = [NCO] \times [Epoxy] \times A_6 \times e^{-\frac{Ea_6}{RT}} \quad \text{Eq.12}$$

Where

r_1 is the model reaction expression use in the model for Eq.1.

It's equal to allophante generation rate

r_2 is the model reaction expression use in the model for Eq.6.

It's equal to oxazolidone generation rate

A_1 and Ea_1 are the Eq.1 reaction pre-exponential factor and activation energy

A_2 and Ea_2 are the Eq.6 reaction pre-exponential factor and activation

These rate expressions are based on Flory's assumption that the inherent reaction rate per functional group is independent of chain length and are based on the concentration of reactive moieties rather than concentration of compounds.[19] The rate expressions of equations 11 and 12 can be modified to reflect changes in isocyanate moiety concentration by multiplying the equations times a stoichiometric coefficient of -1 for each reaction resulting in equations 13 and 14.

$$-\frac{d[NCO]}{dt} = [NCO] \times [Urethane] \times A_1 \times e^{-\frac{Ea_1}{RT}} \quad \text{Eq.13}$$

$$-\frac{d[NCO]}{dt} = [NCO] \times [Epoxy] \times A_6 \times e^{-\frac{Ea_6}{RT}} \quad \text{Eq.14}$$

The modeling of these reactions is based on the solution of Ordinary Differential Equations (13 and 14) using Matlab's ODE45 solver. In this solution, the Arrhenius terms are expressed as reaction rate constants for an isothermal reaction. Two rate constants at two temperatures are then used to solve for the two unknowns of the Arrhenius equations.

2.4 Result and Discussion

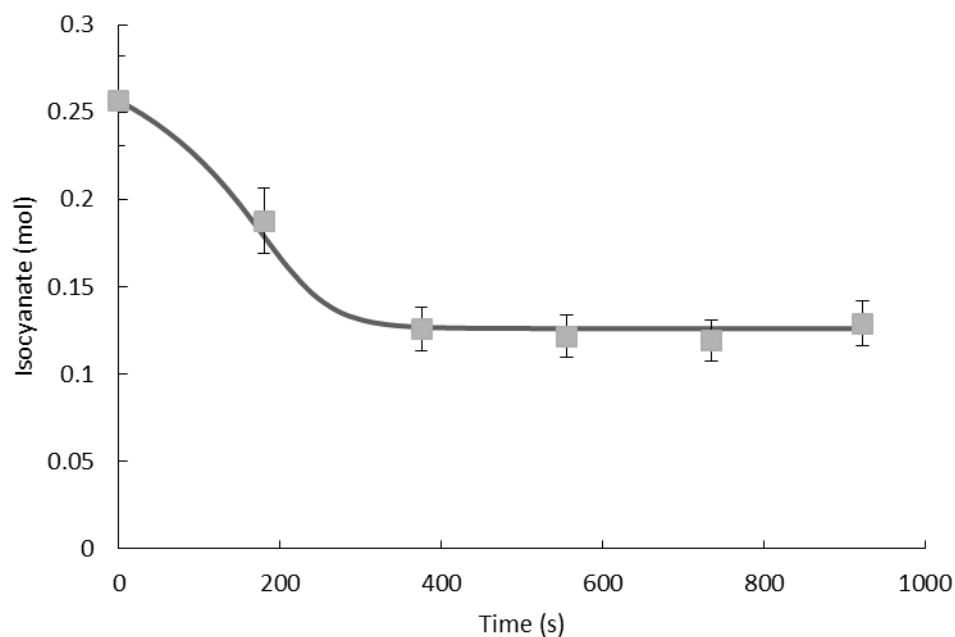


Figure 1. Isocyanate reaction profile with fitted model for reaction of 1-pentanol with PMDI at an isocyanate index =2.0 without catalyst.

The reaction profiles of urethane systems can be characterized into two regimes. The first is where rates are dominated by the reaction between isocyanate and alcohol moieties—Figure 1 illustrates the initial rapid reduction in isocyanate concentration during the first 300 seconds due to this regime.

As illustrated by Figure 1, the model fits the isocyanate concentration data during the first 15 minutes of reaction within the standard deviation of the isocyanate titration concentration profiles. The final value of isocyanate concentration approaches a relatively constant value at about half the initial isocyanate concentration which is consistent with an isocyanate index of 2.0. The fit of the data is based on reaction

parameters previously published which did not require modification which shows in Table3 and Table.4. [18] .

The second regime applies to systems with excess isocyanate and is dominated by reactions between isocyanate and urethane moieties—for the time frame of Figure 1 this reaction had negligible impact. Commercial urethane reaction processes are typically designed around having adequate reactivity during the first two minutes of reaction to set the polymer—this is achieved through use of catalysts.

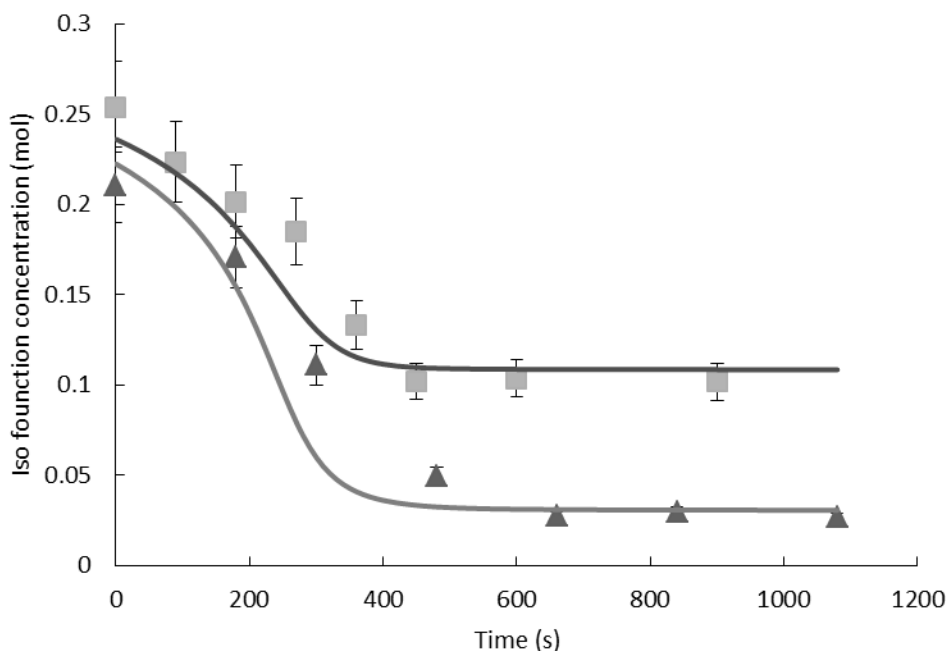


Figure 2. Isocyanate reaction profile with fitted model for reaction of 2-pentanol with PMDI at two isocyanate indices isocyanate indices. Symbols “▲” and “■” represent average experiment data of isocyanate indices of 1.1 and 2.0.

The isocyanate reaction profiles for 2-pentanol are summarized by Figure 2. The fits to the data are reasonable and illustrate the same trends as with 1-pentanol. At longer times the final isocyanate concentrations are reflective of the isocyanate index where at

indices of 2.0 and 1.1 with concentrations are 50% and 9% of the initial concentrations, respectively. The model fits for Figure 2 are based on the use of previously reported reaction parameters for this reaction with Dimethylcyclohexylamine catalyst as summarized by the Table 1 recipe.

Table 3. Kinetic parameters of main reaction without catalysis which has been justified.

	K ml/(mol*s*g catalyst)	E(J/mol)	H (J/mol)
Primary	28	39000	68000
Secondary	12	42000	68000
Hindered Secondary	0.85	54000	68000

Table 4. Kinetic parameters of main reaction with cat8 (Dimethylcyclohexylamine) which has been justified.

	K ml/(mol*s*g catalyst)	E(J/mol)	H(J/mol)
Primary	500	37000	68000
Secondary	55	40000	68000
Tertiary	42	40000	68000

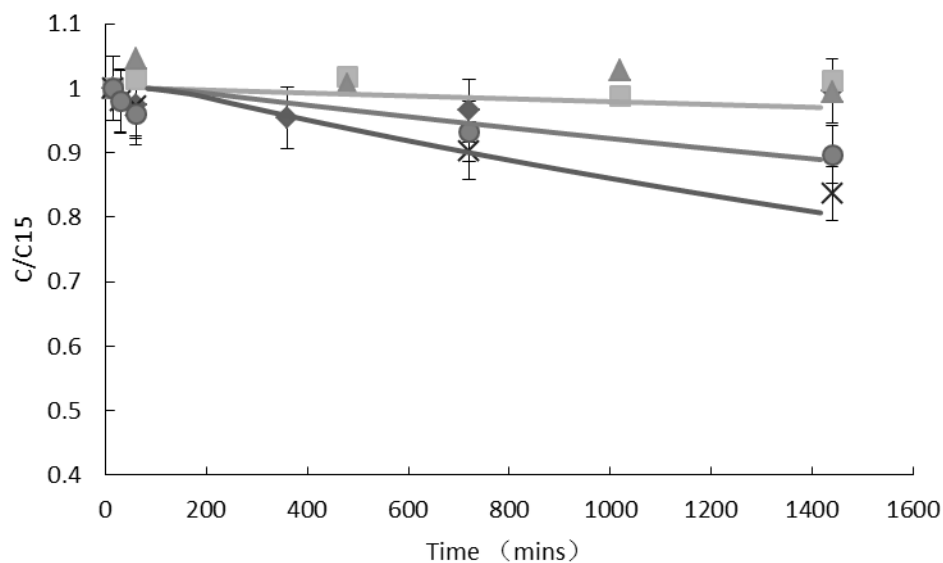


Figure 3. Extended time isocyanate reaction profile with fitted model for reaction of 1-pentanol with PMDI at 80 °C with different catalysts. C_{15} is the concentration of isocyanate functional groups after 15 min of reaction. Symbols “▲”, “■”, “●”, “×” and “◆” represent experiment data with UL22, UL29, Cat5, Cat8 and blank control.

Extended-time studies of the 1-pentanol system are summarized by Figures 3 and 4 at 80 °C and 110 °C where the time scale is in minutes. Model curves are superimposed with the kinetic parameters reported in Tables 4 and 5. The models were based on a rate expression that is first order in both isocyanate and urethane moiety concentrations. The tertiary amine catalyst has the greatest influence on this reaction; the tin catalyst has minimal impact.

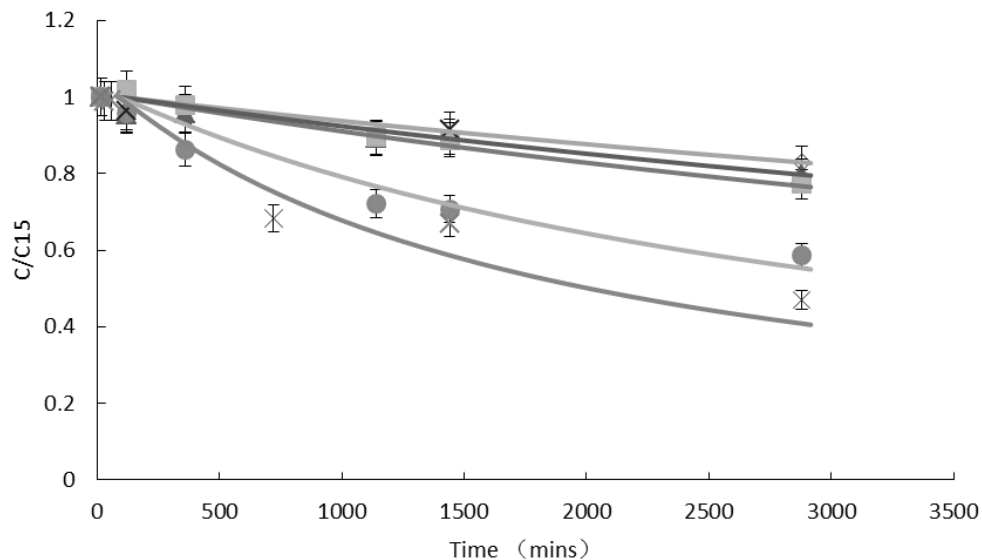


Figure 4. Isocyanate reaction profile with fitted model for reaction of 1-petanol with PMDI at 4 catalysts at 110 °C. Symbols “▲”, “■”, “●”, “×” and “◆” represent experiment data with UL22, UL29, Cat5, Cat8 and blank control.

Table 5 compares the rate constants as reported by Roger [20] to those of this study.

The extended-time isocyanate studies are consistent with what has been reported in literature where conversions in excess of 20% occur at 110 °C and more than 10 hours of reaction.

Table 5. Kinetic parameters of urethane functional groups reaction with isocyanate functional group.

	Isocyanate Index	k ml/(mol*s *g catalyst)	E (J/mol)	Conversion of final at T =395K	k at T =363K	k ml/(mol*s*g catalyst) at T =303K
Control	2.0	0.0006	45000	12.0%	0.0155	0.0008
Cat 8	2.0	0.05	40000	33.4%	0.8980	0.0652
Cat5	2.0	0.02	42000	27.3%	0.4150	0.0264
UL29	2.0	0.008	40000	19.0%	0.1437	0.0108
UL29¹	2.0	0.05	40000	27.3%	0.8980	0.0675
UL22	2.0	0.004	40000	15.9%	0.0718	0.0054
Literature value						
[20]	12.6	-	-	-	-	0.01
[6]	1.6	-	-	5.2%	-	-
[7]	1.0	-	-	10%*	-	-
[8]	3.0	-	-	-	0.83	-

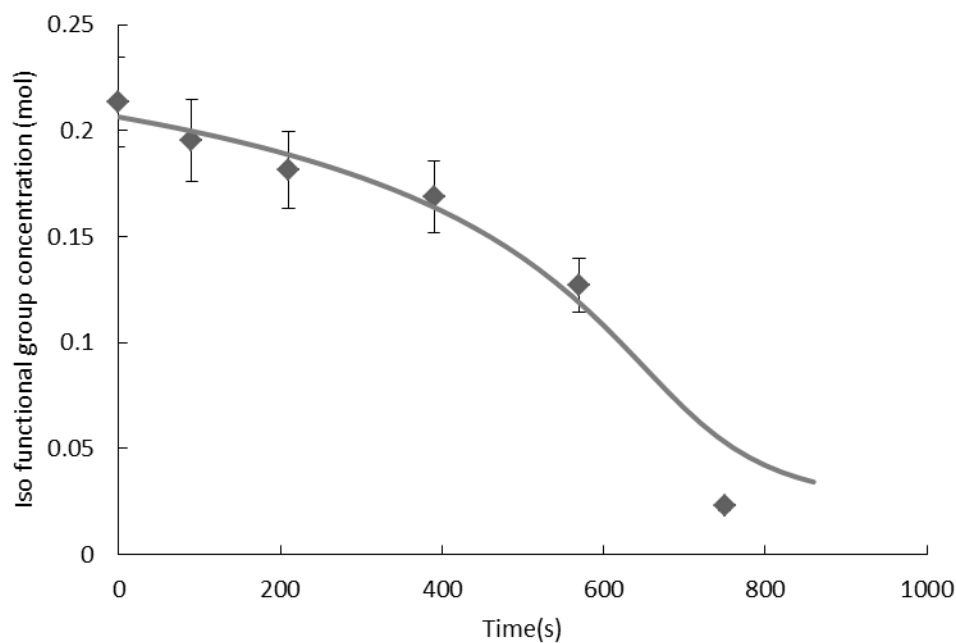


Figure 5. Isocyanate reaction profile with fitted model for reaction of V360 with PMDI at an isocyanate index=1.1 with a catalyst of cat8 at 0.12gram.

For typical urethane-forming systems, polyols are used as reagents rather than simple alcohols like 1- and 2- pentanol. Figures 4 and 5 summarize reaction profiles for reactions of Voranol 360 and polyol 76-635 with PMDI.

As with the simple alcohols, the reaction parameters as previously determined from temperature profiles effectively describe the isocyanate reaction profile for Voranol 360 except at conversions greater than about 50%. At these higher conversions, the polymer begins to set with very high viscosities transitioning to solid polymers. An artifact of isocyanate titrations after about 50% conversion is that the titration provides concentrations that are consistently lower than the model projections. The model results are believed to be a more accurate representation due to the inability of the titrant to access the isocyanate in the solid polymer. Even extensive effort to crush and mix the solid polymer would not provide a better fit to the model at the higher conversions.

A primary reason for use of the 1 and 2 pentanol reaction studies was to avoid issues related to titrating inaccessible isocyanate moieties present in urethane polymers.

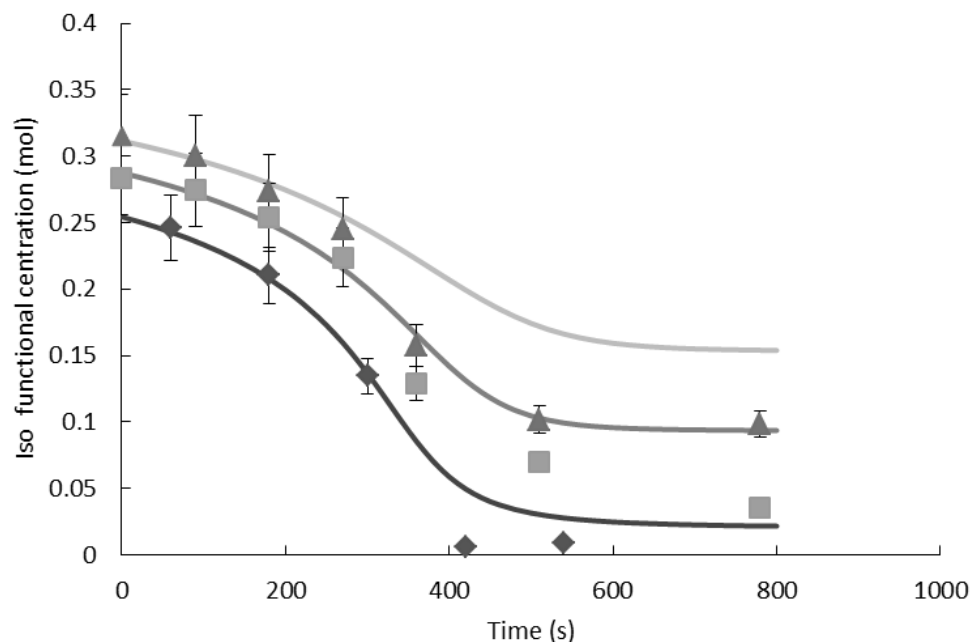


Figure 6. Isocyanate reaction profile with fitted model for reaction of 76-635 with PMDI at three isocyanate indices. Symbols “▲”, “■” and “◆” represent experiment data with isocyanate index=2.0, 1.5 and 1.1.

As illustrated by the isocyanate profiles of Figure 6, Polyol 76-635 exhibits the same trends as Voranol 360 with good agreement between the model and data at lower conversions. The model is able to accurately account for changes in isocyanate index at values between 1.1 and 2.0. Steric hindrance of the analytical method (titration) results in consistent underestimation of isocyanate concentrations after about 50% conversion. The data presented here builds upon previous work where the previous results were based on temperature profiles rather than isocyanate concentration profiles.

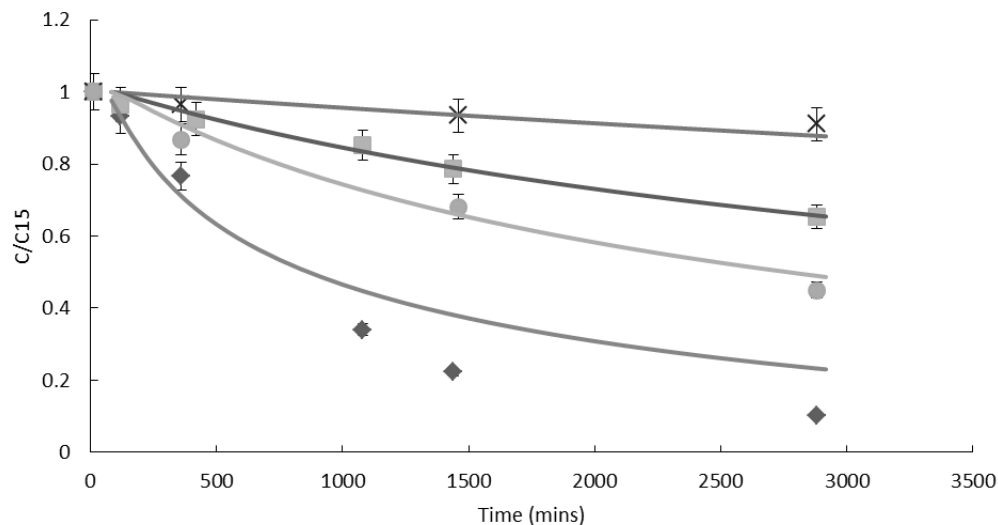


Figure 7. Isocyanate reaction profile with fitted model for reaction of 1-petanol and Epoxy oil with PMDI at different temperature. Symbols “x” and “■” represent experiment data of reaction without any catalyst at 80oC and 110oC. “●” and “◆” represent experiment data with Cat8 at 80oC and 110oC.

Figure 7 shows the experiment and modeling fitting result of the urethane formulation in the presence of epoxidized soybean oil and Cat8 catalyst. Tables 5 and 6 provide the kinetic parameters modeling the impact of temperature based on the Arrhenius equation.

A comparison of the Figure 7 profiles with those of Figures 3 and 4 and the rate constants at specified temperatures of Tables 5 and 6 illustrate that isocyanates have a greater tendency to react with epoxies than with urethanes. This provides evidence that epoxy monomers in a urethane formulation can lead to increased crosslinking as a result of reactions that occur during the hours and days after the initial setting of the urethane polymer.

For gel reactions with epoxy present at 80°C, the viscosity of the mixture was observed to continuously increase during the 48 hours of reactions. At 110°C the system

remained liquid when no catalyst was used but formed a solid elastomer in the presence of Cat 8. No gels were observed for the reaction mixtures at similar conditions in the absence of epoxy moieties (ie where isocyanates reacted with urethanes).

From a polymer device engineering perspective, an adequate amount of alcohol moiety must be present to set the polymer, but after the polymer is set the epoxy can impact properties and enhance performance (for certain applications) during a curing period of hours and days.

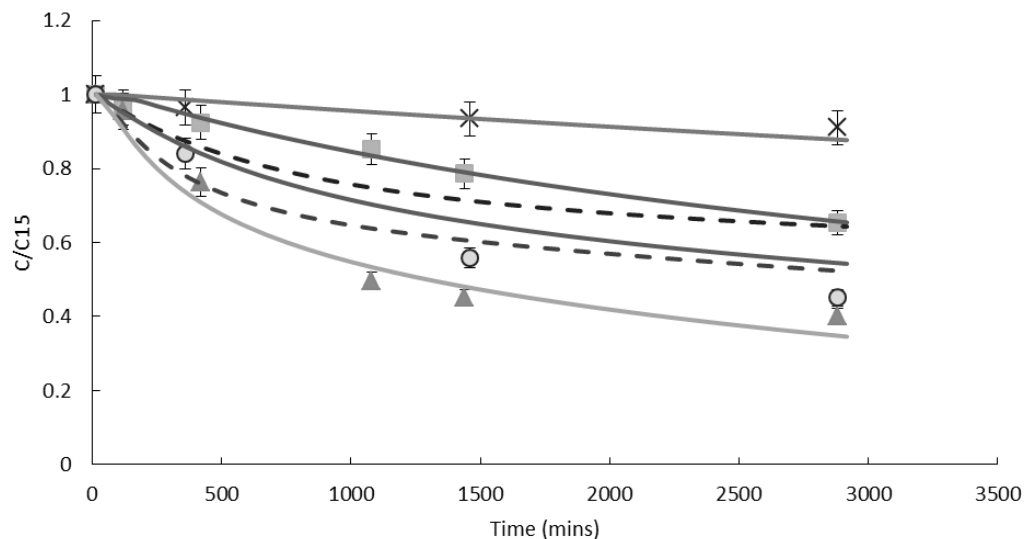


Figure 8. Isocyanate reaction profile with fitted model for reaction of 1-pentanol and Epoxy oil with PMDI at different temperature. Symbols “x” and “■” represent experiment data of reaction without any catalyst at 80°C and 110°C. “●” and “▲” represent experiment data with Cat8 at 80°C and 110°C. Dash line represent model without acceleration.

Catalyst UL 29, also, effectively catalyzed the reaction of epoxy with isocyanate. Figure 8 demonstrates the tin catalyst was effective in accelerating the reaction with epoxy. When compared to the isocyanate-urethane reaction, the tin catalyst had a greater propensity to impact the epoxy reaction. Tin catalysts are known to be effective with epoxy resins. A possible explanation is a reaction mechanism including a complex of the tin catalyst with the epoxy moiety. One could hypothesize that many of the catalysts effective for forming epoxy resins would also be effective for allowing epoxy monomers to participate in urethane-forming processes.

An interesting artifact of the data of Figure 8 is that the conversions associated with the addition of epoxy moieties to the reaction system may exceed what is possible with the amount of epoxy added to the system. Figure 4 illustrates that at 3000 minutes,

allophanate formation can be attributed to a change of up to 0.24 in the C/C15 ratio at 110 °C. The ratio of epoxy to isocyanate moieties (based on the recipe) can lead to a maximum change of about 0.3 in the C/C15 ratio. In view of this, if the isocyanate conversion at 100 C with Cat8 is due to reaction with epoxy moieties, essentially all of the epoxy has reacted.

Tables 3 through 6 summarize the kinetic parameters used by the model to estimate reaction profiles. The results have a good consistency with what has been previously reported[17]. Within experimental error, the reactivity of the isocyanate moieties with urethane moieties are independent of whether the isocyanate is on PMDI or on a urethane polymer.

The results indicate that within the time frames of urethane foaming processes the impact of the allophanate-forming reaction is negligible. As a result, the generation of heat and increased degree of polymerization that are possible with this reaction can be ignored in the foaming simulation during the timeframe when the polymer is set. During curing time, increased crosslinking could impact properties and performance if excess isocyanate is used in the formulation.

Table 6. Kinetic parameters of epoxy functional groups reaction with isocyanate functional group.

	Isocyanate Index	Catalyst quantity (%)	k ml/(mol*s*g catalyst)	E(J/mol)	k ml/(mol*s*g catalyst)at T =303.15K
Control	2.0	0%	0.001	60000	0.0015
Cat 8	2.0	0.2%	0.06	60000	0.0894
UL29	2.0	0.09%	1.8	30000	2.2000
Literature value[15]					
BDMA	0.5	1%	-	43000	0.0017

2.5 Conclusion

Experimental studies on isocyanate reaction profiles in urethane-forming reaction systems verified previously reported reaction parameters. Allophanate-forming reactions have a negligible impact on heat generation and degree of polymerization during the first three minutes of reaction typical for urethane processing; however, their formation can impact the polymer structure in the hours after the initial urethane-forming processes. Reactions of isocyanates with epoxy moieties were observed to have a minor impact in the <3 minute timeframe and do have significant impacts on crosslinking, including gel formation during longer timeframes. Data indicate that catalysts commonly used in epoxy resin setting reactions (e.g. tin catalysts) tend to promote reactions of epoxies with other moieties present in urethane-forming systems.

When commercial polyol reagents were studied, >50% conversion of the isocyanate moieties rendered some of the isocyanate moieties inaccessible to titration analysis as a means to follow reaction. Cat8, a tertiary amine catalyst, was the most effective catalyst for these systems

2.6 Acknowledgements

The authors thank the United Soybean Board for financial support of the experimental studies used to validate the modeling work.

Chapter 3. Resin from natural oil

3.1 Introduction

Chemicals derived from fossil fuels are not renewable and can lead to air pollution above and beyond what is attainable with use of natural oil feed stocks.

The use and study of natural oils, primarily triglycerides, predates the use of petroleum-based chemicals that now dominate the world of chemical infrastructure. A first natural oil used in the industrial was called drying or semi-drying oil. A drying oil hardens to a tough, solid film after a period of exposure to air. Typical example is Tung oil. It is widely applied in many fine coating for wood.

During the past decade, the natural vegetable oils for use as feedstocks for producing polyols for use in urethanes has emerged as a sustainable industry. Natural vegetable oils are defined as esters of fatty acids and glycerol which originate from plant material. They are mainly composed of triglycerides, an ester which is created from three fatty acids and glycerol. The high triglyceride content of vegetable oils and carbon-carbon double bond makes them an excellent alternative polymer source. Carbon-carbon double bond can cause polymerization directly or indirectly. Some conjugate carbon-carbon double bond have strong reactivity and can react via free radical polymerization or anionic polymerization. Non-conjugate double bonds can be modified to make them more susceptible to take part in polymerization.

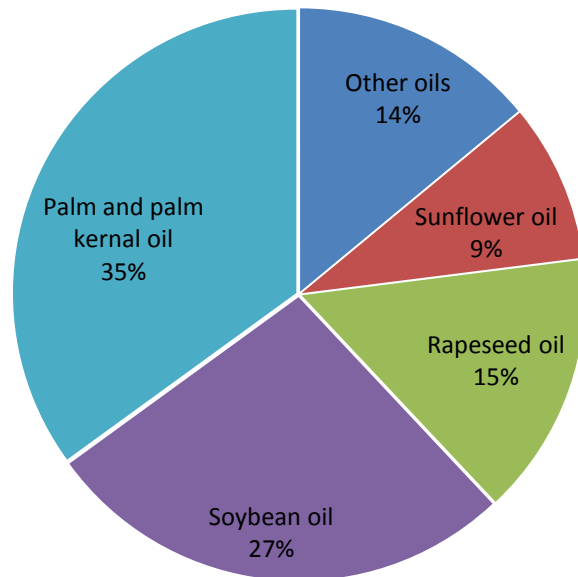
Fatty acids are the source of carbon-carbon double bonds in triglycerides; therefore, the fatty acid composition of a triglyceride is a critical characteristic that defines the reactivity of a natural vegetable oil. Due to high ricinoleic acid, linoleic acid (18:2) and/or

linolenic acid (18:3) contents, castor oil and linseed oil have found many valuable applications based on resin polymerization.

While soybean oil does not have as much linolenic acid as linseed oil (see Table 6), research, it has a high linoleic acid content. This high linoleic acid provides an opportunity for improved chemistry and methods to provide the incremental improvement that is needed to make it useful in the coatings and natural-resins industry.

Figure 9 provides a summary of the dominant global vegetable oil production. Of these dominant oils, soybean oil stands out as having both a high production volume and good susceptibility to resin polymerization.

Global Vegetable Oil Production(2011)
100%=154 million tonnes



Source : Food and Agriculture Organization of the United Nations;

Figure 9. Market volume by kinds.

For vegetable oil polymerization via carbon double bond reaction, the result always generate thermosetting polymer. Generally, the reaction needs heating and stirring to initiate. Free radical chemical initiators can also initiate the reaction.

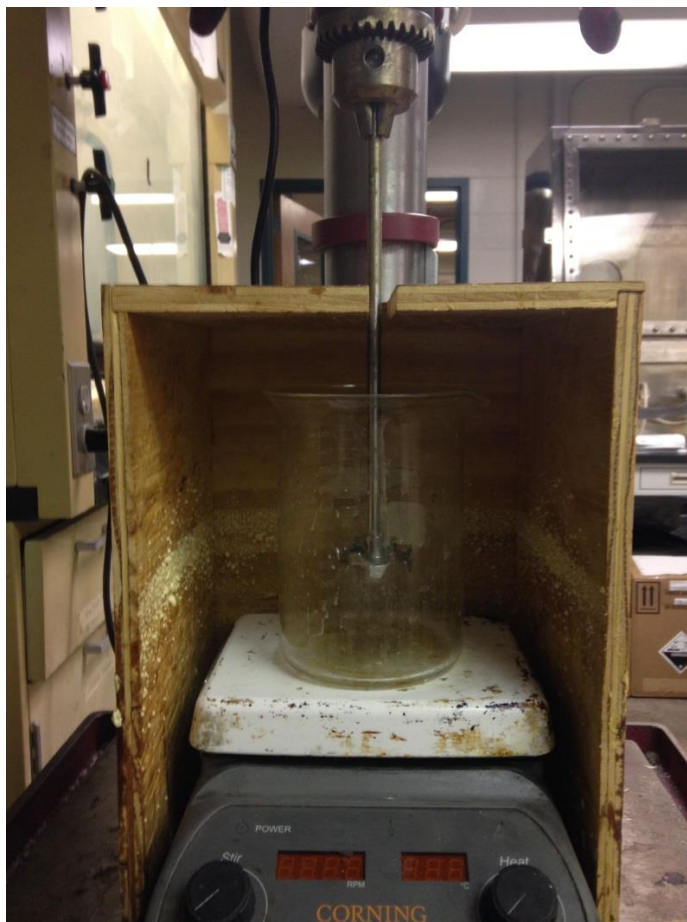


Figure 10. Typical lab experiment polymerization device.

3.2 Background – Natural Oils

Table 7 provides typical vegetable oil fatty acid contents. Table 8 provides a key relating the common fatty acid name to the number of carbons and double bonds of in the fatty acid (e.g. 18:2 indicates 18 carbons and 2 carbon-carbon double bonds. Figures 11 through 14 provide structures of several triglycerides.

Table 7. Typical fatty acid compositions of selected plant oil.^a[21]

Carbon atoms: Double bonds	8:0	10:0	12:0	14:0	16:0	16:1	18:0	18:1	18:2	18:3	20:0	20:1	22:0	22:1	24:0	Iodine value range
Canola oil				0.1	4.0	0.3	1.8	60.9	21.0	8.8	0.7	1.0	0.3	0.7	0.2	100-115
Castor oil					2.0		1.0	7.0	3.0							81-91
Coconut oil	7.1	6.0	46.1	18.5	9.1		2.8	6.8	1.9	0.1	0.1					7-12
Corn oil				0.1	10.9	0.2	2.0	25.4	59.6	1.2	0.4		0.1			118-128
Cottonseed oil			0.1	0.7	21.6	0.6	2.6	18.6	54.4	0.7	0.3		0.2			98-118
Linseed oil					6.0		4.0	22.0	16.0	52.0	0.5					>177
Olive iuk					9.0	0.6	2.7	80.3	6.3	0.7	0.4					76-88
Palm oil			0.1	1.0	44.4	0.2	4.1	39.3	10.0	0.4	0.3		0.1			50-55
Plan kernel oil	3.3	3.4	48.2	16.2	8.4		2.5	15.3	2.3		0.1	0.1				14-19
Peanut oil				0.1	11.1	0.2	2.4	46.7	32.0		1.3	1.6	2.9		1.5	84-100
Rapeseed oil				0.1	3.8	0.3	1.2	18.5	14.5	11.0	0.7	6.6	0.5	41.1	1.0	100-115
Safflower oil				0.1	6.8	0.1	2.3	12.0	77.7	0.4	0.3	0.1	0.2			140-150
Soybean oil				0.1	10.6	0.1	4.0	23.3	53.7	7.6	0.3		0.3			123-139
Sunflower oil				0.1	7.0	0.1	4.5	18.7	18.7	0.8	0.4		0.7			125-140

^aSome oil compositions may not add to 100% due to the presence of minor fatty acides.

^bContains 87% OH-bearing ricinoleic acid (C18:1).

Table 8. Typical fatty acid compositions compare form.

Fatty Acid	#C:#DB	Fatty Acid	#C:#DB
Myristic	14:0	Linolenic	18:3
Palmitic	16:0	Arachidic	20:0
Palmitoleic	16:1	Gadoleic	20:1
Stearic	18:0	Eicosadienoic	22:0
Oleic	18:1	Erucic	22:1
Linoleic	18:2	Lignoceric	24:0

#C: Number of carbon in fatty acid.

#DB: Number of carbon in fatty acid.

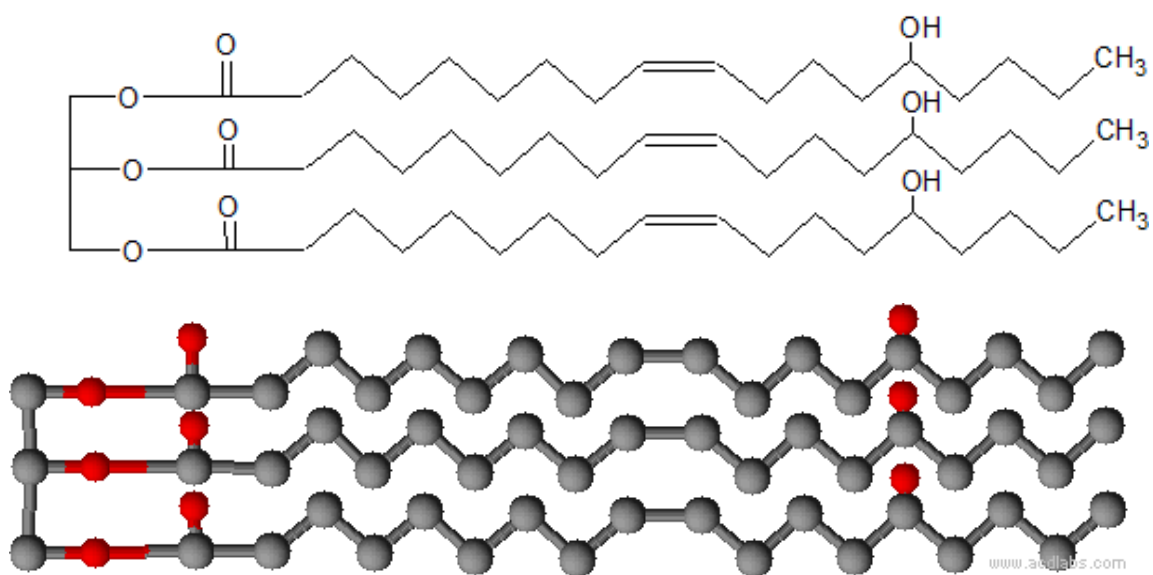


Figure 11. Caster oil (triricinolein).

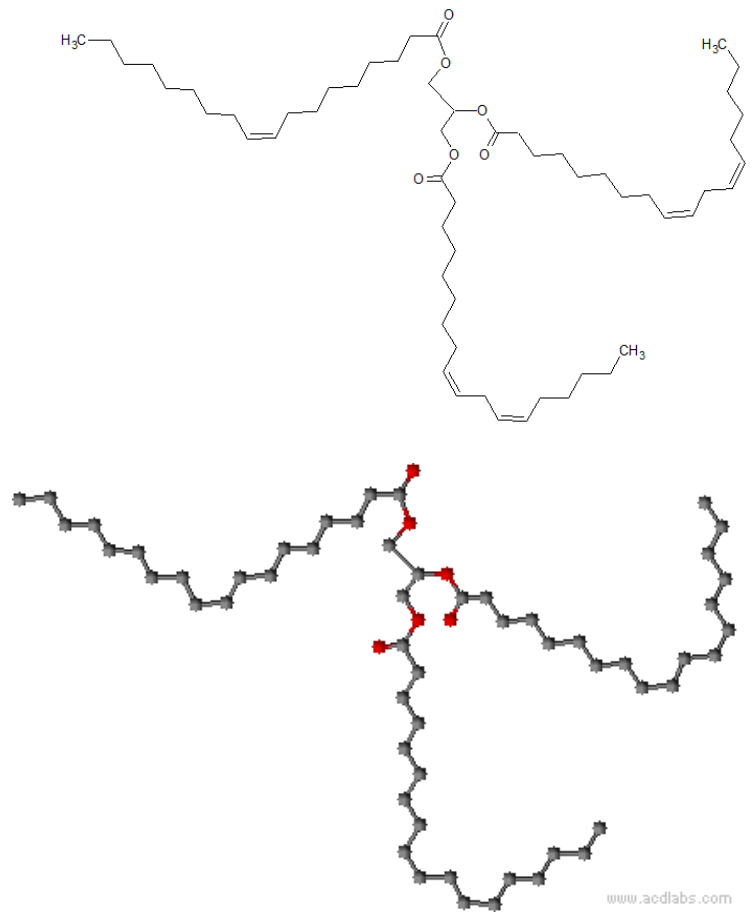


Figure 12. Soybean oil.

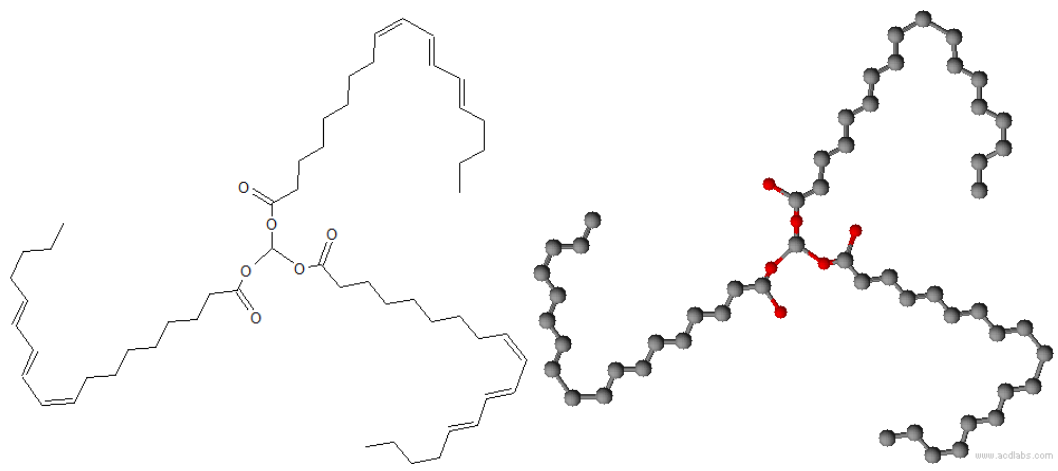


Figure 13. Tung oil [22].

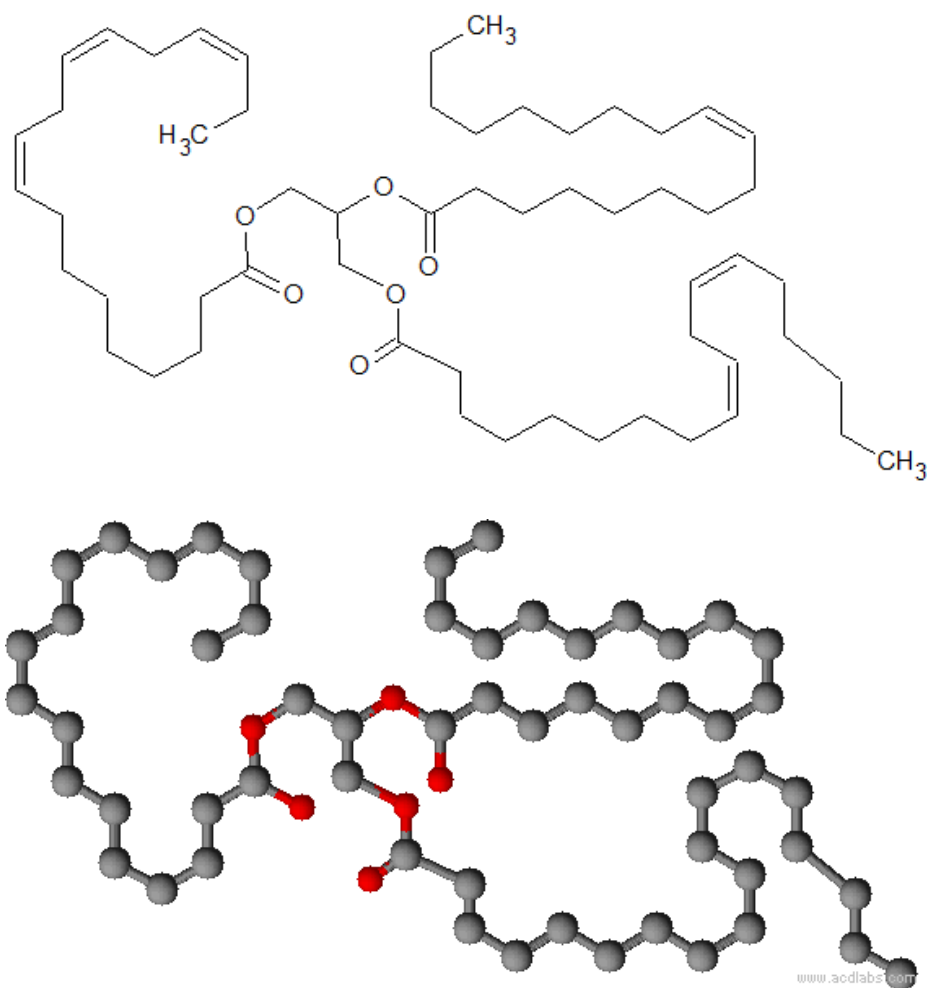


Figure 14. Linseed oil.

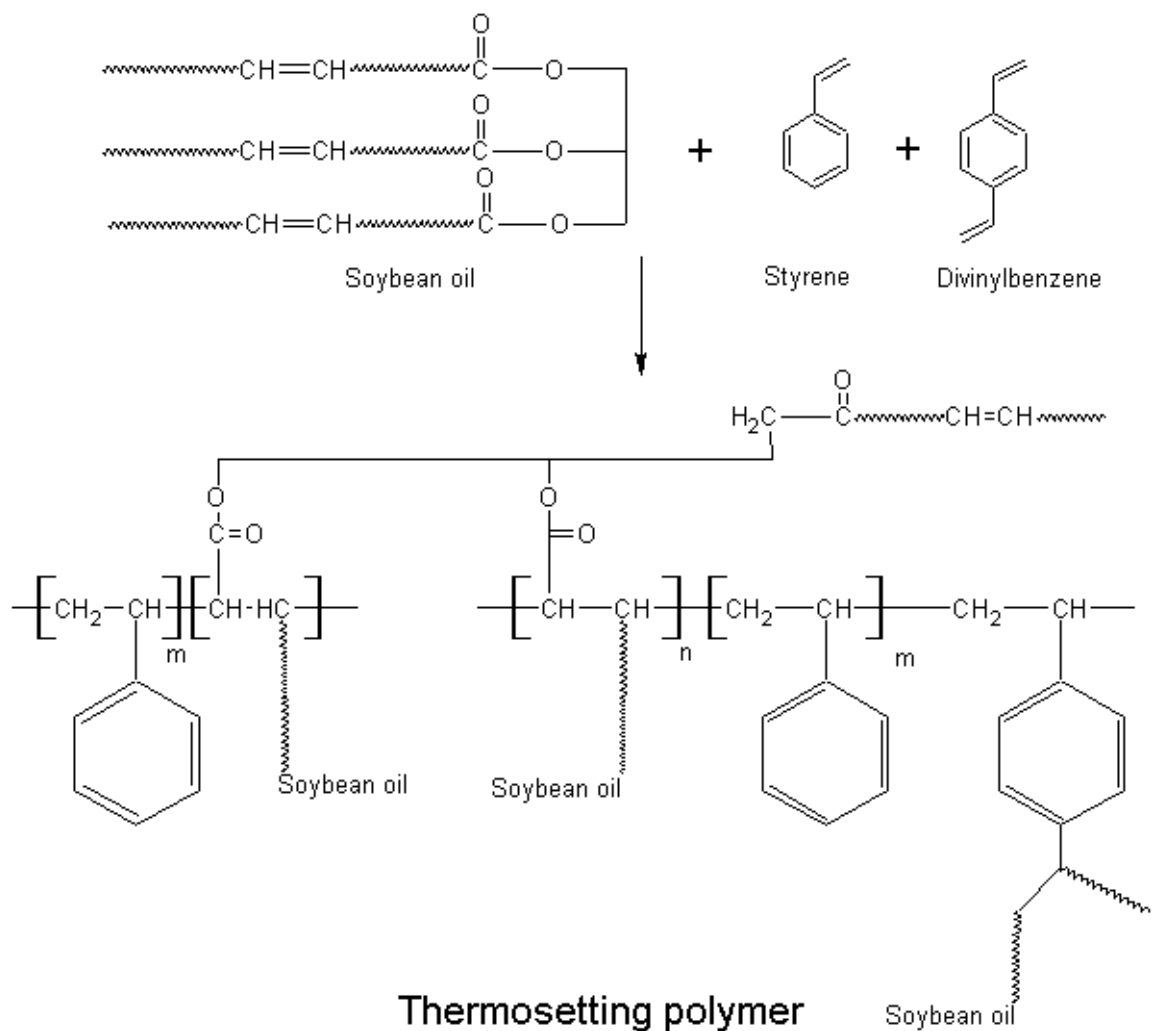


Figure 15. Example polymer structures[23].

3.3 Background – Natural Resin Polymerization

Nature oils contain internal C=C double bonds have the capability to polymerization directly. The double bond can be polymerized through a free radical or a cationic mechanism[24, 25]. Table 9 provides typical catalysts for these polymerizations.

Table 9. Catalysts used by the experiment.

	Prepare process	Polymerization process
Free-radical	Rhodium-based catalysts	-
Cationic	-	BF ₃
		OEt ₂ (BFE)
Hydrosilylation	-	Co(I), Rh(I), Pd(0) or Pt(0)

Free-radical polymerization of triglyceride double has historically received little attention in research because of chain-transfer processes the impact polymer properties. Free radical chain transfer has been considered as the most probable mechanism in some kinds of vegetable such as linseed and tung oil which have been widely used in paints and coatings.

Rhodium-based catalysts can be used to prepare conjugated linseed oil (CLIN) and conjugated low-saturation soybean oil (CLS). These conjugated vegetable oils can subsequently be copolymerized with styrene (ST), acrylonitrile (AN), dicyclopentadiene (DCPD) and divinylbenzene (DVB).[26]

Unsaturated fatty acid chains can participate in the cationic reaction and through a secondary reaction a crosslinked three-dimensional polymer network can be formed. A branch of thermosets polymer create by cationic copolymerization includes reactions of soybean, sunflower, olive, peanut, canola, corn, walnut, and linseed oils using S. Lewis

acids have been used to co-polymerize with vinyl monomers cationically under relatively mild reaction conditions. BF₃.OEt₂ (BFE) is a most efficient catalyst and is commonly used in cationic polymerization of alkenes. Table 10 provides a list of the monomers often used in this copolymerization approach.

Table 10. Summary of typical monomers and applications.

Monomer	Copolymer	Industrial	Experiment
Tung oil	Styrene(ST)	√	√
Castor oil	Acrylonitrile(AN)	√	√
Linseed oil	Dicyclopentadiene(DCPD)	√	√
Soybean oil	Divinylbenzene(DVB)	√	√
Olive oil			√
Peanut oil			√
Canola oil			√
Corn oil			√
Sunflower oil			√

Larock's[27] group reported on studying cationic polymerization of carbon-carbon double bonds and the preparation of thermosetting polymers ranging from rubbers to hard plastics by the cationic copolymerization of a variety of oils with petroleum-based monomers such as styrene, divinylbenzene and dicyclopentadiene in the presence of boron trifluoride diethyl etherate as the initiator.

Another method for vegetable polymerization directly is using Si compounds as copolymers. One is the hydrosilylation reaction. Marina Galià's[28] and Berh's [29] group is study on synthesis new organic organocinorganic hybrid materials via a hydrosilylation reaction. The reaction known as hydrosilylation proceeds when certain hydrosilanes have been activated. They undergo addition across the carbon-carbon multiple bonds. This reaction usually requires a catalyst, the most commonly used of which are the transition metal complexes [Co(I), Rh(I), Pd(0) or Pt(0)].

It is well known that the reactivity of terminal/primary C=C is higher than that of internal/secondary ones. Terminal C=C-containing fatty acid derivatives are available from unsaturated fatty acids by metathesis with ethylene or by pyrolysis.[26] Berh's group involved adding a monofunctional silane compound to the double bond, and introducing a certain silicon reagent to the ester or the oil.

Marina Galià's research investigated the hydrosilylation reaction of terminal unsaturated fatty acid esters with several polyfunctional hydrosilylating agents; 1,4-bis(dimethylsilyl)benzene (DMSB), tetrakis (dimethylsilyloxy) silane (TKDS) and 2,4,6,8-tetramethylcyclotetrasiloxane (TMCTS). These were catalyzed by H₂PtCl₆ in 2-propanol solution (Speier's catalyst) and Pt(0)-divinyltetramethyldisiloxane complex (Karstedt catalyst). The resulting cured hybrid networks showed good transparency as attributed to the good miscibility of the organic and inorganic components. Zengshe's group polymerized soybean oils initiated by boron trifluoride diethyl etherate in supercritical carbon dioxide medium. Results show that the longer reaction time, up to 3 h, favored the higher molecular weight of polymers at conditions of 140°C and initiator BF₃·OEt₂. The resulting polymers had molecular weight ranging from 21,842 to 118,300 g/mol.[30]

3.4 Simulation of Polymerization

In oil resin polymerization, the reactive moiety is the carbon-carbon pi (double) bond. Each carbon-carbon double bond has a functionality of two. Different types of carbon-carbon double bonds in triglyceride have significantly different reactivities. [31]

Equations 11- 13 provide illustrate three categories of double bonds which will be used to lump different reactivities.

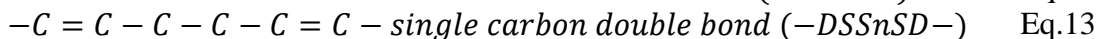
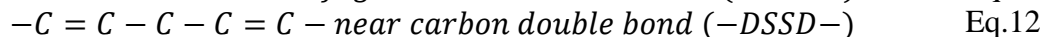
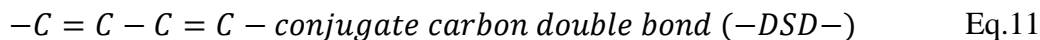


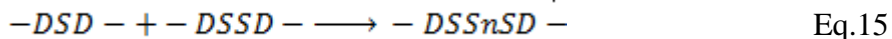
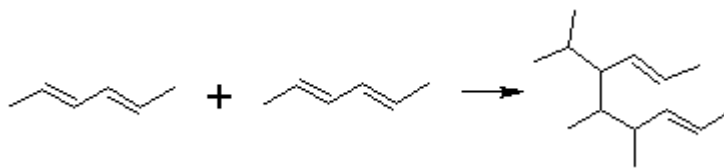
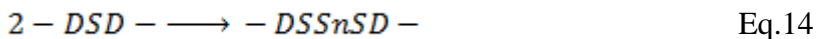
Table 11 provides a summary of the types of these bonds in typical fatty acids founds in the prominent triglycerides.

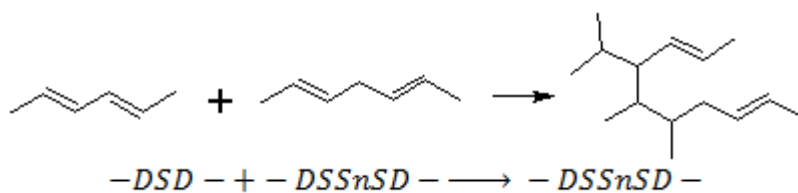
Table 11. Classified fatty acid.

Fatty Acid	#C:#DB	Bond type	Fatty Acid	#C:#DB	Bond type
Myristic	14:0	No double bond	Linolenic	18:3	-DSD-
Palmitic	16:0	No double bond	Arachidic	20:0	No double bond
Palmitoleic	16:1	-DSSnSD-	Gadoleic	20:1	-DSSnSD-
Stearic	18:0	-No double bond	Eicosadienoic	22:0	No double bond
Oleic	18:1	-DSSnSD-	Erucic	22:1	-DSSnSD-
Linoleic	18:2	-DSSD-	Lignoceric	24:0	No double bond

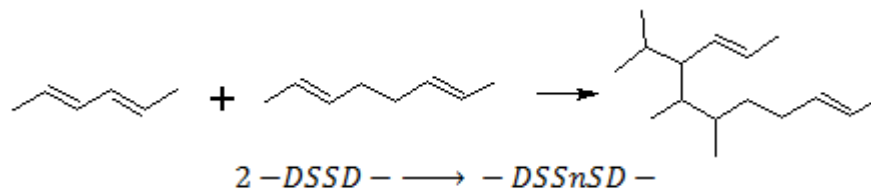
Equations 14-19 provide the reactions that these different types of double bonds can undergo. By hypothesizing these reactions as elementary, these reactions provide both a basis for deriving kinetic expressions and an accounting of how different double bonds react and form in the network of reactions.

3.5 Equation using in Matlab

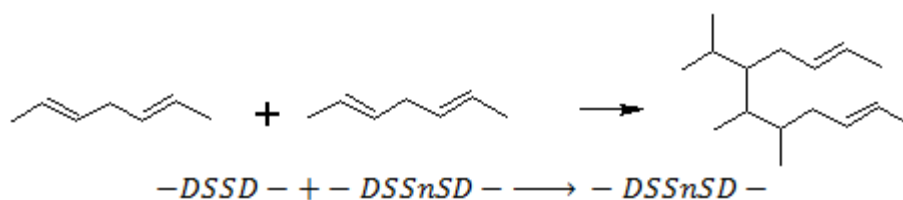




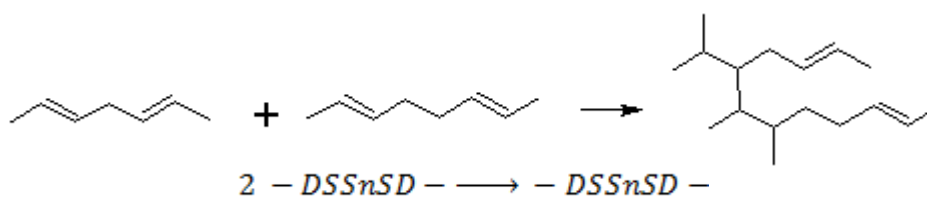
Eq.16



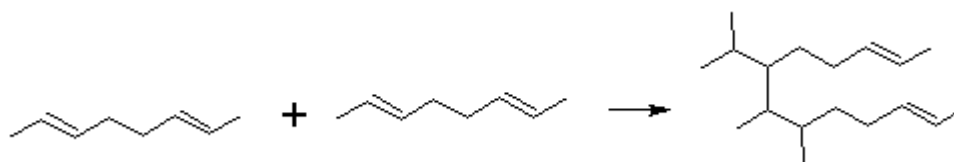
Eq.17



Eq.18



Eq.19



This network of reactions was reduced to a Matlab code for modeling and simulation purposes using the algorithm of Figure 16. The algorithm is designed to provide initial conditions and kinetic information to the OilReac function that defines the ordinary differential equations that result from these reactions under the hypothesis that these are elementary reactions. The actual simulation code is provided by Table 12.

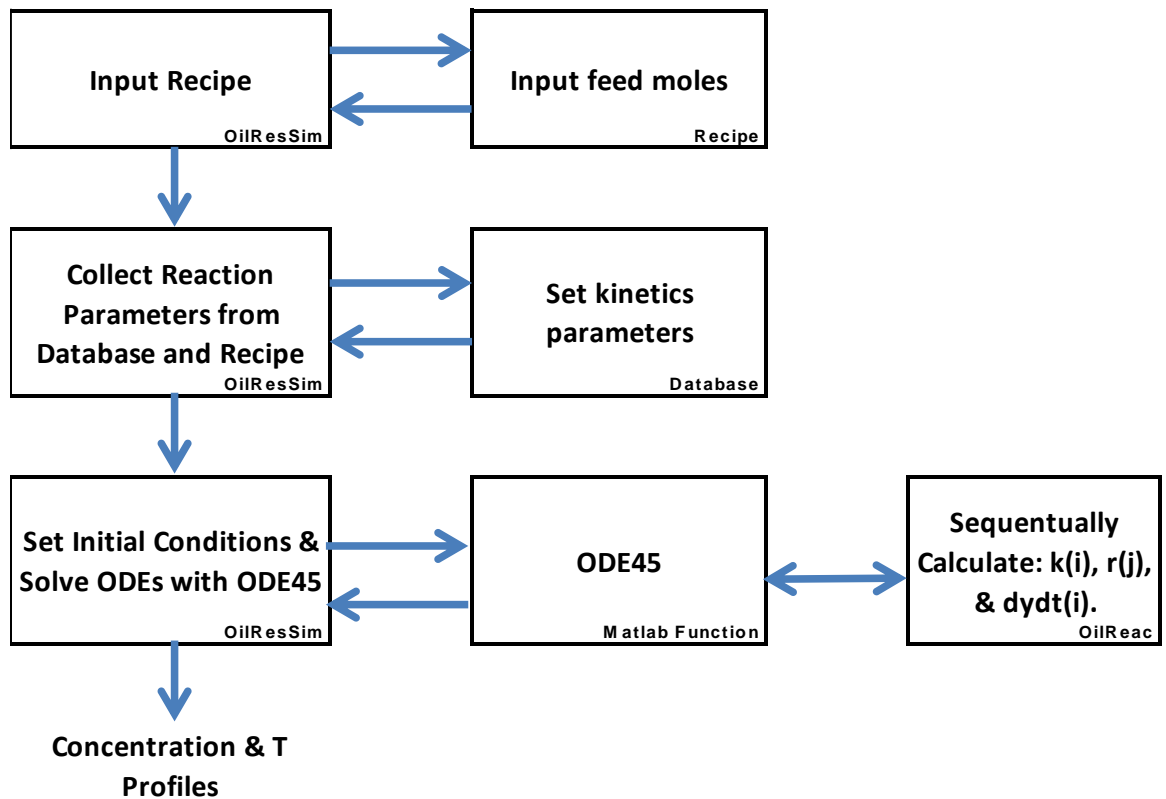


Figure 16. Program algorithm.

Table 12. Simulation code.

```

clear;clc;close all;
global Np1 Np2 fp1 fp2 density1 density2 density3 T0 V X1c X2c X1n X2n X1s X2s Additive
Database
[t,c]=ode45(@OilResSim,[0:10:410],[Np1;Np2;0;Np1*fp1*X1c+Np2*fp2*X2c;Np1*fp1*X1n+Np2*fp2*X2n;
Np1*fp1*X1s+Np2*fp2*X2s;298]);
%V=100/density1+100/density2; %%constant
V=c(:,1)/density1+c(:,2)/density2+c(:,3)/density3; %%changing
figure
plot(t,c(:,1))
hold on
plot(t,c(:,2),'r')
hold on
plot(t,c(:,3),'g')
title('Mole of monomer changing with time')
xlabel('Time(s)')
ylabel('Mole')
legend('Soybean oil','Copolymer','Polymer')
figure
plot(t,c(:,4))
hold on
plot(t,c(:,5),'r')

```

```

hold on
plot(t,c(:,6),'g')
title('Mole of carbon double bond changing with time')
xlabel('Time(s)')
ylabel('Mole')
legend('-DSD-', '-DSSD-', '-DSSnSD-')
figure
plot(t,c(:,7)-273.15)
DP=(c(1,1)+ c(1,2)+c(1,3))/( c(:,1)+ c(:,2)+ c(:,3));
title('Temperature changing with time')
xlabel('Time(s)')
ylabel('Degrees Celsius')
figure
plot(t,DP)
title('Degree of polymerization(DP) changing with time')
xlabel('Time(s)')
ylabel('DP')

```

```

function Database
global Mp1 Mp2 fp1 fp2 Np1 Np2 E A h Cp1 Cp2 Cp3 U T0 V X1c X2c X1n X2n X1s X2s Additive
cat density1 density2 density3
Mp1=87.3; %% initial weight of soybean oil
Mp2=10.4; %% initial weight of copolymer

fp1=4; %% Functionality of soybean oil
X1c=0.076/(0.076+0.53+0.234); % conjugate
X1n=0.53/(0.076+0.53+0.234); % near
X1s=0.234/(0.076+0.53+0.234); % single
fp2=2; %% Functionality of copolymer
X2c=1; % conjugate
X2n=0; % near
X2s=0; % single

density1=1;
density2=1;
density3=1;
T0=298;
cat=0;
Additive=0;
Np1=Mp1/872.94; % mol initial concentration of soybean oil
Np2=Mp2/104.15; % mol initial concentration of copolymer

E(:,1)=[48000;0]; % J/mol activation energy of reaction p1 conjugate and p2 conjugate
E(:,2)=[34000;0]; % J/mol activation energy of reaction p1 conjugate and p2 near
E(:,3)=[0;0]; % J/mol activation energy of reaction p1 conjugate and p2 single
E(:,4)=[34000;0]; % J/mol activation energy of reaction p1 near and p2 conjugate
E(:,5)=[0;0]; % J/mol activation energy of reaction p1 near and p2 near
E(:,6)=[0;0]; % J/mol activation energy of reaction p1 near and p2 single
E(:,7)=[0;0]; % J/mol activation energy of reaction p1 single and p2 conjugate
E(:,8)=[0;0]; % J/mol activation energy of reaction p1 single and p2 near
E(:,9)=[0;0]; % J/mol activation energy of reaction p1 single and p2 single
E(:,10)=[48000;0]; % J/mol activation energy of reaction p1 conjugate and polymer conjugate
E(:,11)=[34000;0]; % J/mol activation energy of reaction p1 conjugate and polymer near
E(:,12)=[0;0]; % J/mol activation energy of reaction p1 conjugate and polymer single
E(:,13)=[34000;0]; % J/mol activation energy of reaction p1 near and polymer conjugate
E(:,14)=[0;0]; % J/mol activation energy of reaction p1 near and polymer near
E(:,15)=[0;0]; % J/mol activation energy of reaction p1 near and polymer single
E(:,16)=[0;0]; % J/mol activation energy of reaction p1 single and polymer conjugate
E(:,17)=[0;0]; % J/mol activation energy of reaction p1 single and polymer near
E(:,18)=[0;0]; % J/mol activation energy of reaction p1 single and polymer single
E(:,19)=[48000;0]; % J/mol activation energy of reaction p2 conjugate and polymer conjugate
E(:,20)=[34000;0]; % J/mol activation energy of reaction p2 conjugate and polymer near
E(:,21)=[0;0]; % J/mol activation energy of reaction p2 conjugate and polymer single
E(:,22)=[0;0]; % J/mol activation energy of reaction p2 near and polymer conjugate
E(:,23)=[0;0]; % J/mol activation energy of reaction p2 near and polymer near
E(:,24)=[0;0]; % J/mol activation energy of reaction p2 near and polymer single

```

```

E(:,25)=[0;0]; %J/mol activation energy of reaction p2 single and polymer conjugate
E(:,26)=[0;0]; %J/mol activation energy of reaction p2 single and polymer near
E(:,27)=[0;0]; %J/mol activation energy of reaction p2 single and polymer single
E(:,28)=[48000;0]; %J/mol activation energy of reaction polymer conjugate and polymer conjugate
E(:,29)=[34000;0]; %J/mol activation energy of reaction polymer conjugate and polymer near
E(:,30)=[0;0]; %J/mol activation energy of reaction polymer conjugate and polymer single
E(:,31)=[0;0]; %J/mol activation energy of reaction polymer near and polymer near
E(:,32)=[0;0]; %J/mol activation energy of reaction polymer near and polymer single
E(:,33)=[0;0]; %J/mol activation energy of reaction polymer single and polymer single
E(:,34)=[30000;0]; %J/mol activation energy of reaction polymer single and polymer single
E=[E(:,1), E(:,2), E(:,3), E(:,4), E(:,5), E(:,6), E(:,7), E(:,8), E(:,9), E(:,10), E(:,11),
E(:,12), E(:,13), E(:,14), E(:,15), E(:,16), E(:,17),E(:,18), E(:,19), E(:,20), E(:,21),
E(:,22), E(:,23), E(:,24), E(:,25), E(:,26), E(:,27), E(:,28), E(:,29), E(:,30), E(:,31),
E(:,32), E(:,33),E(:,34)];

```

```

A(:,1)=[3;0]; %Reaction rate p1 conjugate and p2 conjugate
A(:,2)=[1;0]; % Reaction rate p1 conjugate and p2 near
A(:,3)=[0;0]; % Reaction rate p1 conjugate and p2 single
A(:,4)=[1;0]; % Reaction rate p1 near and p2 conjugate
A(:,5)=[0;0]; % Reaction rate p1 near and p2 near
A(:,6)=[0;0]; % Reaction rate p1 near and p2 single
A(:,7)=[0;0]; % Reaction rate p1 single and p2 conjugate
A(:,8)=[0;0]; % Reaction rate p1 single and p2 near
A(:,9)=[0;0]; % Reaction rate p1 single and p2 single
A(:,10)=[3;0]; % Reaction rate p1 conjugate and polymer conjugate
A(:,11)=[1;0]; % Reaction rate p1 conjugate and polymer near
A(:,12)=[0;0]; % Reaction rate p1 conjugate and polymer single
A(:,13)=[1;0]; % Reaction rate p1 near and polymer conjugate
A(:,14)=[1;0]; % Reaction rate p1 near and polymer near
A(:,15)=[0;0]; % Reaction rate p1 near and polymer single
A(:,16)=[0;0]; % Reaction rate p1 single and polymer conjugate
A(:,17)=[0;0]; % Reaction rate p1 single and polymer near
A(:,18)=[0;0]; % Reaction rate p1 single and polymer single
A(:,19)=[3;0]; % Reaction rate p2 conjugate and polymer conjugate
A(:,20)=[1;0]; % Reaction rate p2 conjugate and polymer near
A(:,21)=[0;0]; % Reaction rate p2 conjugate and polymer single
A(:,22)=[0;0]; % Reaction rate p2 near and polymer conjugate
A(:,23)=[0;0]; % Reaction rate p2 near and polymer near
A(:,24)=[0;0]; % Reaction rate p2 near and polymer single
A(:,25)=[0;0]; % Reaction rate p2 single and polymer conjugate
A(:,26)=[0;0]; % Reaction rate p2 single and polymer near
A(:,27)=[0;0]; % Reaction rate p2 single and polymer single
A(:,28)=[2;0]; % Reaction rate polymer conjugate and polymer conjugate
A(:,29)=[0.5;0]; % Reaction rate polymer conjugate and polymer near
A(:,30)=[0;0]; % Reaction rate polymer conjugate and polymer single
A(:,31)=[0;0]; % Reaction rate polymer near and polymer near
A(:,32)=[0;0]; % Reaction rate polymer near and polymer single
A(:,33)=[0;0]; % Reaction rate polymer single and polymer single
A(:,34)=[3;0]; % Reaction rate polymer single and polymer single
A=[A(:,1), A(:,2), A(:,3), A(:,4), A(:,5), A(:,6), A(:,7),A(:,8),A(:,9),A(:,10),A(:,11),
A(:,12),A(:,13), A(:,14),A(:,15),A(:,16),A(:,17),A(:,18),A(:,19),A(:,20),A(:,21),A(:,22),A(:,23),A(:,24),
A(:,25),A(:,26),A(:,27),A(:,28),A(:,29),A(:,30),A(:,31),A(:,32),A(:,33),A(:,34)];

```

```

h=[70000,70000]; %J/mol heats of reactions: p1 react with p2; p2 react with p2
Cp1=300;
Cp2=200;
Cp3=400; % %polymer cp

```

U=1;

```

function dydt= OilResSim(t,c)
global Mp1 Mp2 fp1 fp2 Np1 Np2 Cp1 Cp2 Cp3 U density1 density2 density3 E A h T0 X1c
X2c X1n X2n X1s X2s cat ;

```

```

V=Mp1/density1+Mp2/density2+c(3)/density3;
Cp=c(1)*Cp1+c(2)*Cp2+c(3)*Cp3;
for i=1:34
k(i)=A(1,i)*exp(E(1,i)/8.3145*(1/298-1/c(7)))+A(2,i)*cat*exp(E(2,i)/8.3145*(1/298-1/c(7)));
end;

```

```

V=100/density1+100/density2;
P1c=fp1*X1c*c(1);
P1n=fp1*X1n*c(1);
P1s=fp1*X1s*c(1);
P2c=fp2*X2c*c(2);
P2n=fp2*X2n*c(2);
P2s=fp2*X2s*c(2);

PcP=c(4)+c(5)-(P1c+P2c);
PnP=c(4)+c(5)-(P1n+P2n);%0
PsP=c(4)+c(5)-(P1s+P2s);%0

r=[
k(1)*P1c*P2c/V^2; % P1 conjugate with P2 conjugate
k(2)*P1c*P2n/V^2; % P1 conjugate with P2 near
k(3)*P1c*P2s/V^2; % P1 conjugate with P2 single
k(4)*P1n*P2c/V^2; % P1 near with P2 conjugate
k(5)*P1n*P2n/V^2; % P1 near with P2 near
k(6)*P1n*P2s/V^2; % P1 near with P2 single
k(7)*P1s*P2c/V^2; % P1 single with P2 conjugate
k(8)*P1s*P2n/V^2; % P1 single with P2 near
k(9)*P1s*P2s/V^2; % P1 single with P2 single
k(10)*P1c*PcP/V^2; % P1 conjugate with polymer conjugate
k(11)*P1c*PnP/V^2; % P1 conjugate with polymer near
k(12)*P1c*PsP/V^2; % P1 conjugate with polymer single
k(13)*P1n*PcP/V^2; % P1 near with polymer conjugate
k(14)*P1n*PnP/V^2; % P1 near with polymer near
k(15)*P1n*PsP/V^2; % P1 near with polymer single
k(16)*P1s*PcP/V^2; % P1 single with polymer conjugate
k(17)*P1s*PnP/V^2; % P1 single with polymer near
k(18)*P1s*PsP/V^2; % P1 single with polymer single
k(19)*P2c*PcP/V^2; % P2 conjugate with polymer conjugate
k(20)*P2c*PnP/V^2; % P2 conjugate with polymer near
k(21)*P2c*PsP/V^2; % P2 conjugate with polymer single
k(22)*P2n*PcP/V^2; % P2 near with polymer conjugate
k(23)*P2n*PnP/V^2; % P2 near with polymer near
k(24)*P2n*PsP/V^2; % P2 near with polymer single
k(25)*P2s*PcP/V^2; % P2 single with polymer conjugate
k(26)*P2s*PnP/V^2; % P2 single with polymer near
k(27)*P2s*PsP/V^2; % P2 single with polymer single
k(28)*PcP*PcP/V^2; % polymer conjugate with polymer conjugate
k(29)*PcP*PnP/V^2; % polymer conjugate with polymer near
k(30)*PcP*PsP/V^2; % polymer conjugate with polymer single
k(31)*PnP*PnP/V^2; % polymer near with polymer near
k(32)*PnP*PsP/V^2; % polymer near with polymer single
k(33)*PsP*PsP/V^2; % polymer single with polymer single
k(34)*PsP*PsP/V^2]; % P2 self

%   1 2 3 4 5 6 7 8 9 10 11 12 13 14 15 16 17 18 19 20 21 22 23 24 25
26 27 28 29 30 31 32 33
sc=[-1 -1 -1 -1 -1 -1 -1 -1 -1 -1 -1 -1 -1 -1 -1 -1 -1 -1 -1 0 0 0 0 0 0
0 0 0 0 0 0 0 0; % monomer P1
-1 -1 -1 -1 -1 -1 -1 -1 0 0 0 0 0 0 0 0 -1 -1 -1 -1 -1 -1
-1 -1 0 0 0 0 0 0 -2; % monomer P2
1 1 1 1 1 1 1 1 1 1 0 0 0 0 0 0 0 0 0 0 0 0 0 0 0
0 0 -1 -1 -1 -1 -1 -1 1; % Polymer
-2 -1 -1 0 0 -1 0 0 -2 -1 -1 -1 0 0 -1 0 0 -2 -1 -1 -1 0 0 -1
0 0 -2 -1 -1 0 0 0 -2; % Total conjugate
0 -1 0 -1 -2 -1 0 -1 0 0 -1 0 -1 -2 -1 0 -1 0 -1 0 -1 -2 -1 0
-1 0 0 -1 0 -2 -1 0 0; % Total near
1 1 0 1 1 0 0 0 -1 1 1 0 1 1 0 0 0 -1 1 1 0 1 1 0 0
0 -1 1 1 0 1 0 -1 0]; % Total single
%%0 -1 0 -1 -2 -1 0 -1 0 0 -1 0 -1 -2 -1 0 -1 0 0 -1 0 -1 -2 -1 0
-1 0 0 -1 0 -2 -1 0 0; % Total near

dydt=[sc*;
((r(1)+r(2)+r(3)+r(4)+r(5)+r(6)+r(7)+r(8)+r(9)+r(10)+r(11)+r(12)+r(13)+r(14)+

```



```
r(15)+r(16)+r(17)+r(18))*h(1)+(r(19)+r(20)+r(21)+r(22)+r(23)+r(24)+r(25)+r(26)
+r(27)+r(28)+r(29)+r(30)+r(31)+r(32)+r(33)+r(34))*h(2)+0.1*U*(T0-c(7))/Cp%temperature
];
if c(3)<0
    dydt(3)=0;
end
if c(4)<0
    dydt(4)=0;
end
if c(5)<0
    dydt(5)=0;
end
if c(6)<0
    dydt(6)=0;
end
```

3.6 Experimental Studies and Verification of Model

The Table 12 simulation code was written to simulate the resin polymerization of soybean oil using the following composition:

- Carbon-carbon double bond fraction is 15.3%;
- -DSD- fraction is 7.6%;
- -DSSD- fraction is 53.7%;
- -DSSnSD- fraction is 23.4%, and
- Styrene defined as 100% -DSD- double bond.

Reactant A is soybean oil and B is styrene.

For this reaction system, only three reactions are simulated, Seven parameters is related with the experiment result; therefore, seven groups of reactions under different reactant ratios are needed. A soybean oil molecular weight of 872.94 was used. Masses of all components are entered in the recipe function and that total remains constant during reaction.

Table 13. Typical recipe.

Ratio B/A	Reactant A(gram)	Reactant A(mole)	Reactant B(gram)	Reactant B(mole)
1.0	87.3	0.1	10.4	0.1
1.5	82.9	0.094	14.8	0.142
2.0	78.9	0.09	18.8	0.181
2.5	75.3	0.086	22.44	0.216
3.0	72.0	0.082	25.8	0.247
3.5	68.9	0.079	28.8	0.276
4.0	66.1	0.076	31.56	0.303

Published experimental results [32] were used to fit kinetic parameters. Reagents were: soybean oil purchased from a local supermarket, styrene (ST, 99%), DVB (80% mixture of isomers), and BFE (redistilled); the latter purchased from Aldrich Chemical Company and used without further purification. Differential scanning calorimetry was used to follow the reaction conversion. Kinetic parameters are summarized in Table 14. Literature also provide free radical scavenger capacity of oil in lipidic phase at 180 °C[33] as summarized in Table 15.

Table 14. Literature value of soybean oil reaction(Determination of Kinetic Parameters from Dynamic DSC measurement Using Kissinger's Equation).[32]

Initiator (wt %)	Ea(KJ/mol)	ln(A)
1	113±10	24±3
2	68±3	10±1
3	54±9	7±3

Table 15. Free Radical Scavenger Capacity of oil in lipidic phase at 180 °C.[33]

Oil source	$k_T(\text{min}^{-1}) \times 10^{-3}$
Olive	6.5±0.5
Sunflower	4.3±0.2
Corn	2.2±0.1
Rapeseed	3.5±0.2
Soybean	1.7±0.1
Safflower	4.1±0.3

3.7 Simulation results

Simulation results were performed using the kinetic parameters of Table 14. As the Figure 17 illustrates, copolymerization reaction reacts at higher rates than soybean oil alone.

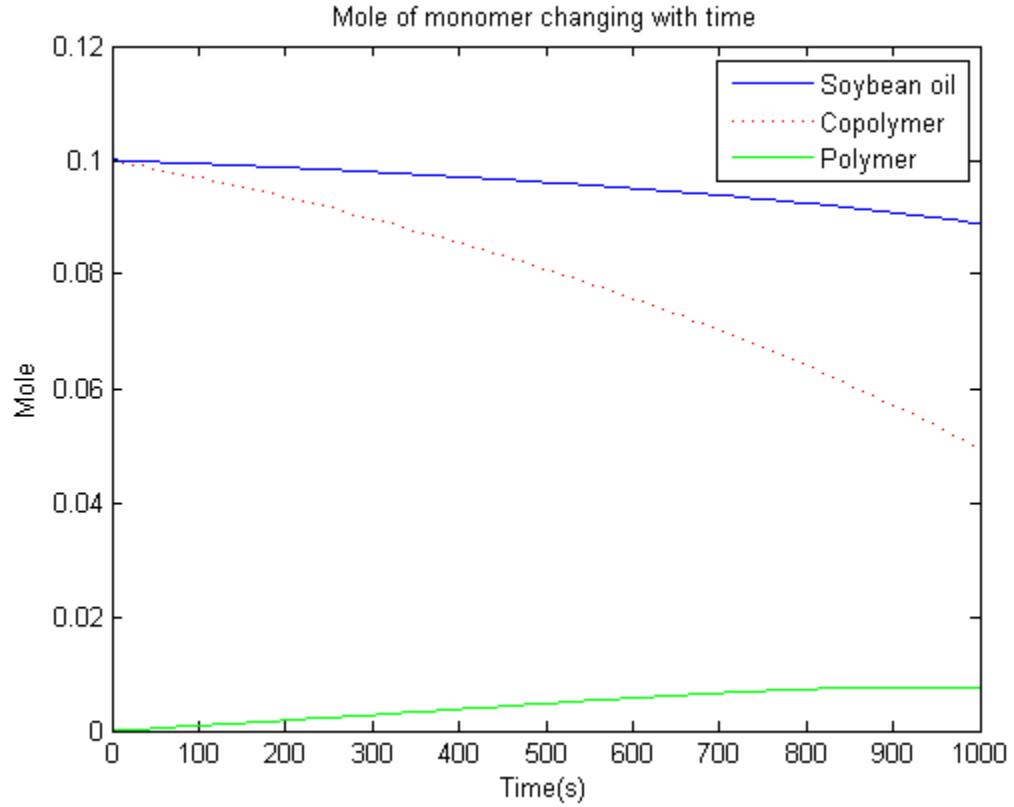


Figure 17. Example simulation output-Monomer profiles.

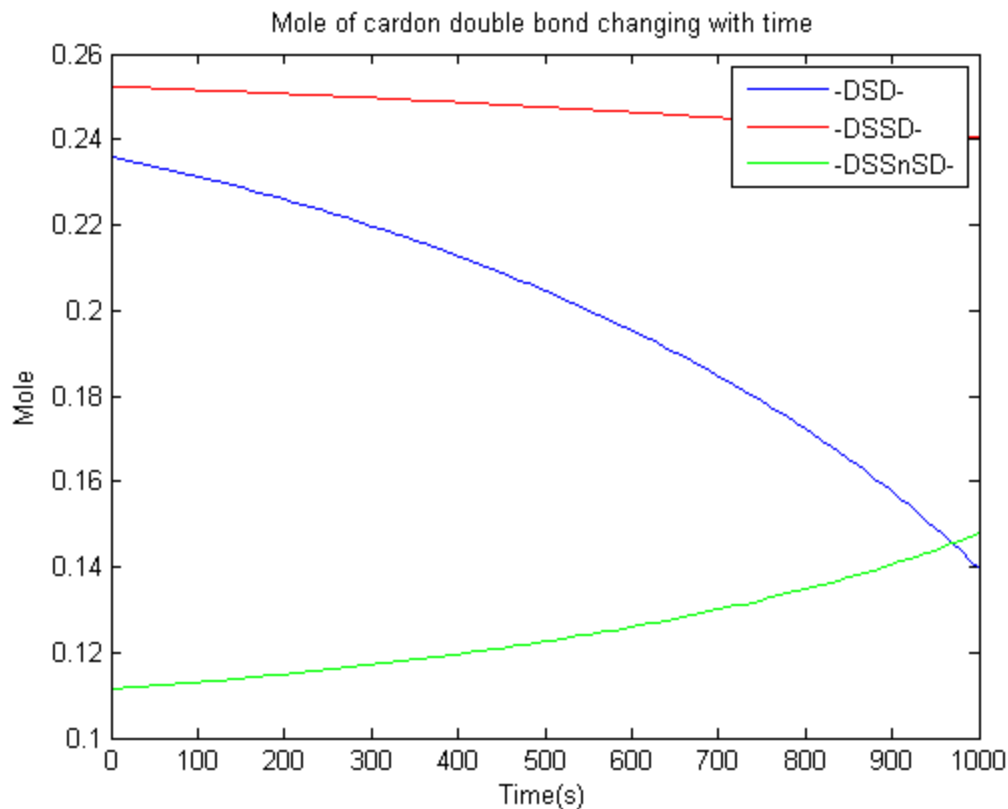


Figure 18. Example simulation output-Carbon-carbon double bonds profiles.

Figure 18 follows the profiles of the different types of double bonds. The reaction is dominated by the reactions of DSD groupings.

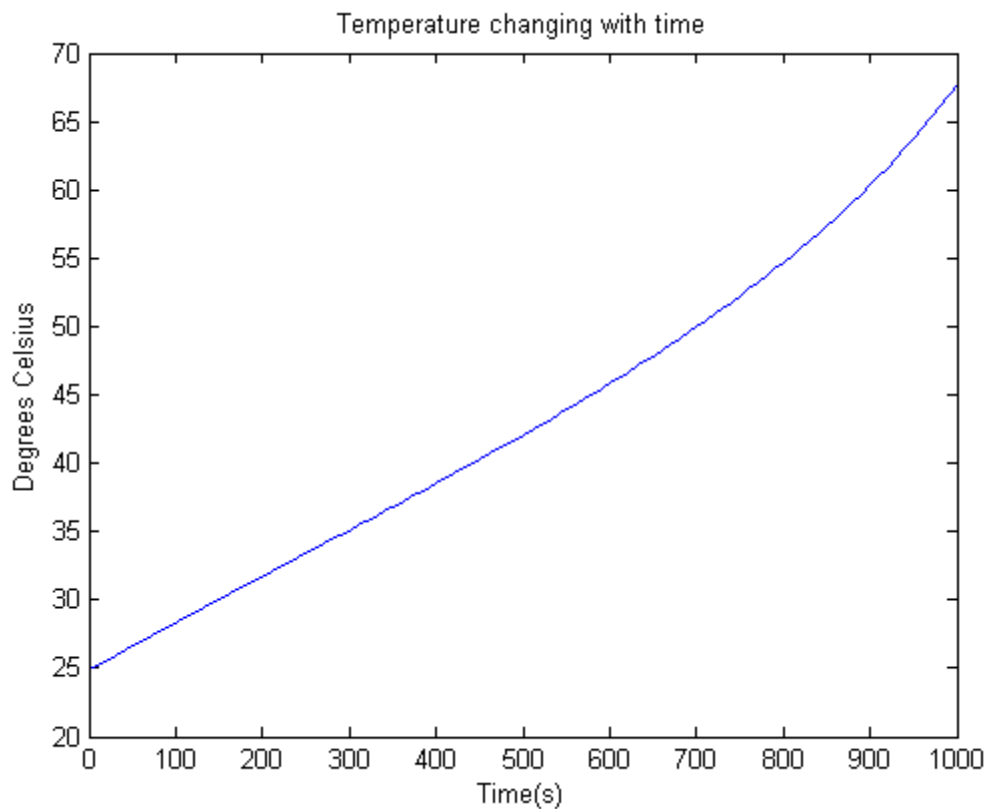


Figure 19. Example simulation output-Temperature profiles.

Figure 19 provides example simulation output of the temperature increase during reaction. The reaction rate is highly dependent on temperature.

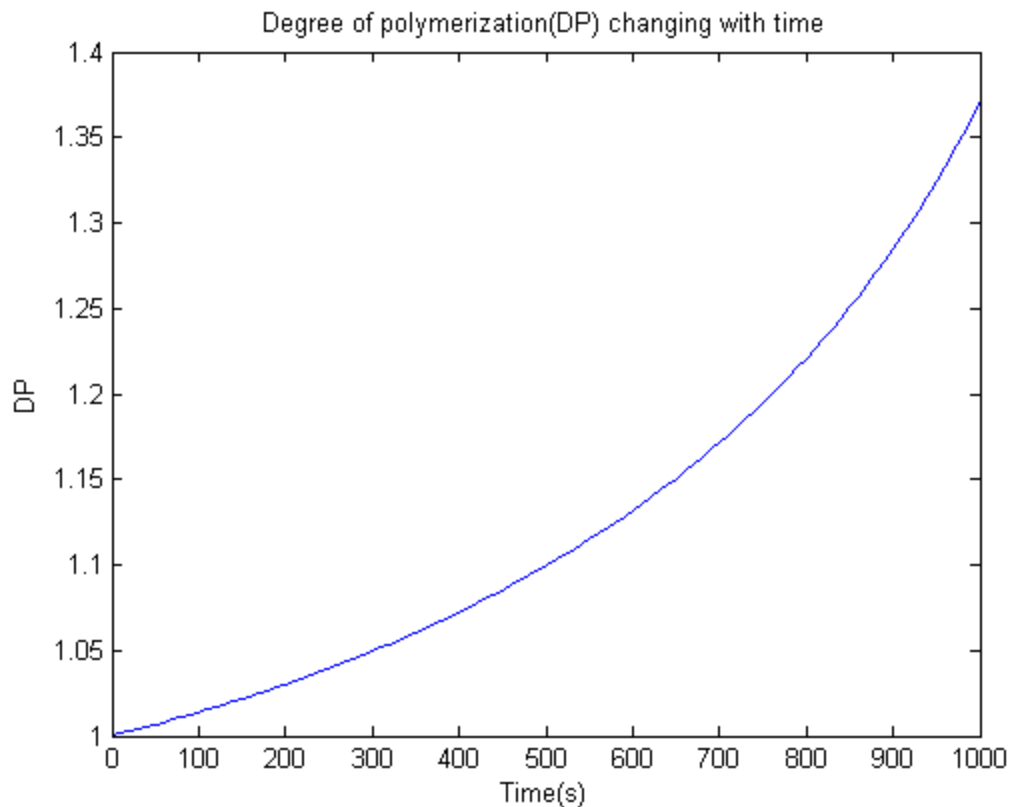


Figure 20. Example simulation output-Degree of polymerization profiles.

Figure 20 illustrates how the degree of polymerization increases during reaction. This system clearly requires further optimization to obtain useful degrees of polymerization. The use of this simulation code could find great utility in to perform this optimization more efficiently and to identify conditions that will likely be successful.

Chapter 4. Future study

The simulation approach presented in this thesis represents a sophisticated and detailed approach to modeling urethane systems as well as resin polymerization. As detailed in the urethane discussions, urethane recipes typically consist of combinations of at least six and up to a dozen reagents, catalyst, surfactants, and other additives. This complex mix of reagents leads to very demanding simulation conditions to present meaningful results.

On the modeling of urethane systems, the following was successfully achieved in this work.

- Modeling and prediction of temperature profiles,.
- Modeling and prediction of isocyanate moiety concentration profiles.
- Modeling of kinetic data for both non-catalytic and catalytic reactions.
- An understanding of reactivity influencing isocyanate and epoxy moiety concentration profiles in urethane systems has been expanded.

On the modeling of resin polymerization systems, the following was successfully achieved in this work.

- A network of fundamentally based reactions has been identified to represent the reacting system.
- A Matlab-based program has been written to simulate the system.
- Model parameters were adjusted to be consistent with published data.

The following are recommended as topics of future work that provide attainable and meaningful advances of the methods presented in this thesis.

- Further verification of reactions in urethane systems including the following of epoxy moiety concentrations.
- Develop a theory of relating the different reactivities of carbon-carbon double bonds including the impact of the size of the molecule to which the bonds are attached.

Bibliography

1. Duff, D.W. and G.E. Maciel, *Carbon-13 and nitrogen-15 CP/MAS NMR characterization of MDI-polyisocyanurate resin systems*. *Macromolecules*, 1990. **23**(12): p. 3069-3079.
2. Singh, P. and J.L. Boivin, *Studies on the stability of the dimer of 2, 4-tolylene diisocyanate*. *Canadian Journal of Chemistry*, 1962. **40**(5): p. 935-940.
3. Querat, E., et al., *Blocked isocyanate. Reaction and thermal behaviour of the toluene 2, 4-diisocyanate dimer*. *Die Angewandte Makromolekulare Chemie*, 1996. **242**(1): p. 1-36.
4. Kogon, I., *Chemistry of Aryl Isocyanates: Rate and Equilibrium Constants for the Formation of Ethyl α , γ -Diarylallophanate*. *The Journal of Organic Chemistry*, 1959. **24**(1): p. 83-86.
5. Schwetlick, K. and R. Noack, *Kinetics and catalysis of consecutive isocyanate reactions. Formation of carbamates, allophanates and isocyanurates*. *J. Chem. Soc., Perkin Trans. 2*, 1995(2): p. 395-402.
6. Heintz, A.M., et al., *Effects of reaction temperature on the formation of polyurethane prepolymer structures*. *Macromolecules*, 2003. **36**(8): p. 2695-2704.
7. Lapprand, A., et al., *Reactivity of isocyanates with urethanes: conditions for allophanate formation*. *Polymer degradation and stability*, 2005. **90**(2): p. 363-373.
8. Špírková, M., M. Kubin, and K. Dušek, *Side Reactions in the Formation of Polyurethanes: Stability of Reaction Products of Phenyl Isocyanate*. *Journal of Macromolecular Science-Chemistry*, 1990. **27**(4): p. 509-522.
9. Vivaldo-Lima, E., et al., *Modeling of nonlinear polyurethane production in batch reactors using a kinetic-probabilistic approach*. *Industrial & engineering chemistry research*, 2002. **41**(21): p. 5207-5219.
10. Delebecq, E., et al., *On the Versatility of Urethane/Urea Bonds: Reversibility, Blocked Isocyanate, and Non-isocyanate Polyurethane*. *Chemical reviews*, 2012. **113**(1): p. 80-118.
11. Dusek, K., M. Spirkova, and I. Havlicek, *Network formation of polyurethanes due to side reactions*. *Macromolecules*, 1990. **23**(6): p. 1774-1781.
12. Lubguban, A.A., et al., *Isocyanate reduction by epoxide substitution of alcohols for polyurethane bioelastomer synthesis*. *International Journal of Polymer Science*, 2011. **2011**.

13. Hsieh, F.-H., et al., *Urethane formulation*. 2012, Google Patents.
14. Okumoto, S. and S. Yamabe, *A computational study of base-catalyzed reactions between isocyanates and epoxides affording 2-oxazolidones and isocyanurates*. Journal of Computational Chemistry, 2001. **22**(3): p. 316-326.
15. Caille, D., J.P. Pascault, and L. Tighzert, *Reaction of a diepoxide with a diisocyanate in bulk*. Polymer Bulletin, 1990. **24**(1): p. 23-30.
16. Morgans Jr, D., K. Sharpless, and S.G. Traynor, *Epoxy alcohol rearrangements: hydroxyl-mediated delivery of Lewis acid promoters*. Journal of the American Chemical Society, 1981. **103**(2): p. 462-464.
17. Rima Ghoreishi, Y.Z., Galen J. Suppes, *Reaction Modeling of Urethane Polyols Using Fraction Primary Secondary, and Tertiary Hydroxyl Content*, in *CPI*. 2013: Phoenix.
18. Zhao, Y., et al., *Modeling reaction kinetics of rigid polyurethane foaming process*. Journal of applied polymer science, 2013.
19. Flory, P.J., *Principles of polymer chemistry*. 1953: Cornell University Press.
20. Van Maris, R., et al., *Polyurethane catalysis by tertiary amines*. Journal of cellular plastics, 2005. **41**(4): p. 305-322.
21. Petrović, Z.S., *Polyurethanes from vegetable oils*. Polymer Reviews, 2008. **48**(1): p. 109-155.
22. Hondred, P.R., et al., *Tung oil-based thermosetting polymers for self-healing applications*. Journal of Applied Polymer Science, 2014.
23. Sharma, V. and P. Kundu, *Addition polymers from natural oils—A review*. Progress in Polymer Science, 2006. **31**(11): p. 983-1008.
24. Bozell, J.J. and M.K. Patel, *Feedstocks for the Future: Renewables for the Production of Chemicals and Materials*. 2006: American Chemical Society Washington, DC.
25. Wool, R.P. and X. Sun, „*Bio-Based Polymers and Composites*”, 2005. New York: Elsevier. Bledzki, AK, and J. Gassan, Prog. Polym. Sci, 1999. **24**: p. 221-274.
26. Farzaneh Mazloumfard, T.M., Ahmed Mehairi, Shahir Mishriki. <http://vegetableoilbasedpolymers.wikispaces.com/4.+Vegetable+Oil+Polymer+Production>.

27. Lu, Y. and R.C. Larock, *Novel polymeric materials from vegetable oils and vinyl monomers: preparation, properties, and applications*. ChemSusChem, 2009. **2**(2): p. 136-147.
28. Lligadas, G., et al., *Novel organic–inorganic hybrid materials from renewable resources: Hydrosilylation of fatty acid derivatives*. Journal of Polymer Science Part A: Polymer Chemistry, 2005. **43**(24): p. 6295-6307.
29. Behr, A., F. Naendrup, and D. Obst, *The synthesis of silicon oleochemicals by hydrosilylation of unsaturated fatty acid derivatives*. European journal of lipid science and technology, 2002. **104**(3): p. 161-166.
30. Liu, Z. and S.Z. Erhan, *Preparation of soybean oil polymers with high molecular weight*. Journal of Polymers and the Environment, 2010. **18**(3): p. 243-249.
31. Seniha Güner, F., Y. Yağcı, and A. Tuncer Erciyes, *Polymers from triglyceride oils*. Progress in Polymer Science, 2006. **31**(7): p. 633-670.
32. Badrinarayanan, P., et al., *Cure characterization of soybean oil—Styrene—Divinylbenzene thermosetting copolymers*. Journal of applied polymer science, 2009. **113**(2): p. 1042-1049.
33. Esp ñ, J.C., C. Soler-Rivas, and H.J. Wichers, *Characterization of the total free radical scavenger capacity of vegetable oils and oil fractions using 2, 2-diphenyl-1-picrylhydrazyl radical*. Journal of Agricultural and Food Chemistry, 2000. **48**(3): p. 648-656.